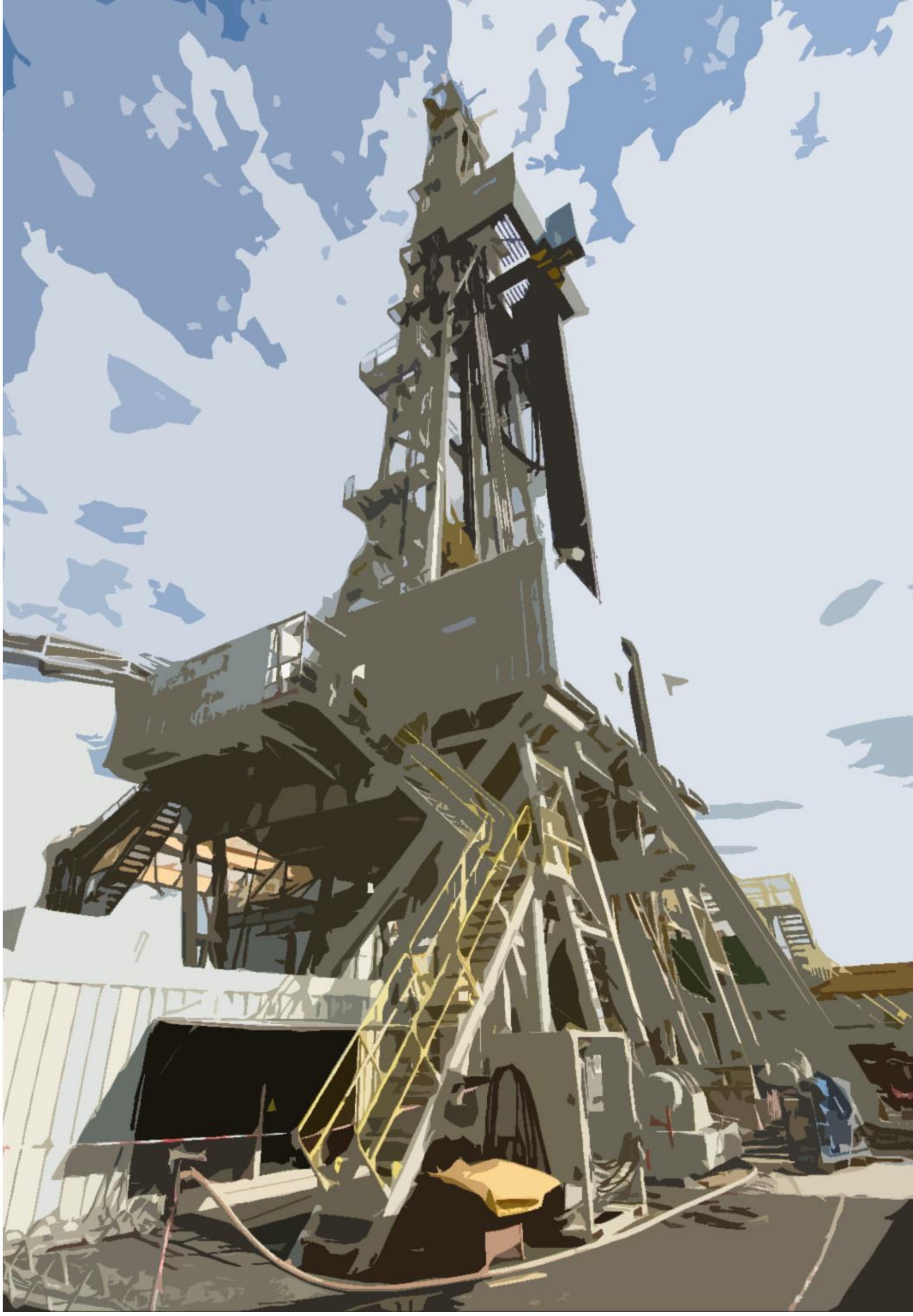

Defining the Framework for Seismic Hazard Assessment in Geothermal Projects V0.1

Technical Report

Report title:	Defining the Framework for Seismic Hazard Assessment in Geothermal Projects V0.1 - Technical Report
Author(s):	Stefan Baisch[1], Christopher Koch[1], Henrik Stang[1], Bas Pittens[2], Benno Drijver[2], Nick Buik[2]
Date:	05.10.2016
Project:	Kennisagenda - Defining the Framework for Seismic Hazard Assessment in Geothermal Projects
Prepared for:	KennisAgenda Aardwarmte (Dutch Geothermal Research Agenda) sponsored by the Ministry of Economic Affairs, LTO Glaskracht Nederland and the program “Kas als Energiebron”.
Version:	161005

[1]Q-con GmbH, Marktstrasse 39, 76887 Bad Bergzabern, Germany

[2]IF Technology B.V., Velperweg 37, 6824 BE Arnhem, The Netherlands

Contents

1 OVERVIEW

To further improve the quality of geothermal energy production and in particular the standards on monitoring and reacting on seismic events, a protocol is presented for the assessment of seismic hazard and risk associated with geothermal systems in the Netherlands. The protocol aims to assist project developers in understanding and mitigating these seismicity risks.

Based on theoretical concepts and a data set of global observations, geological and operational parameters are identified which are considered most relevant for seismic hazard. These provide the fundament of a three-level procedure for addressing seismic hazard and risk.

An initial estimate of the induced seismicity potential is obtained from a Quick-Scan of key parameters (Level 1). If the Quick-Scan indicates a medium or high potential for induced seismicity, a location-specific seismic hazard assessment (Level 2) is required. Based on the results of the SHA, it is decided whether or not a more detailed Level 3 seismic risk assessment is needed. In both cases, local seismic monitoring in combination with a traffic-light-system is recommended.

General guidelines are provided for performing Level 2 and Level 3 assessments.

The proposed protocol is based on information and observations that are currently available (‘evidence based’). Future observations or insights may require modifications or even revisions.

2 INTRODUCTION

Geothermal systems have the potential to provide significant amounts of sustainable energy in the Netherlands. A controversial issue associated with geothermal systems is the occurrence of induced seismicity.

Many conventional geothermal fields in the world have been producing over decades without having caused noticeable seismicity. In a few cases, however, felt earthquakes were associated with geothermal operations. The most prominent example is a magnitude M_w=3.2 earthquake induced by a geothermal reservoir stimulation underneath the city of Basel, Switzerland (Deichmann & Giardini, 2009), which caused minor but widespread damage to buildings (Baisch et al., 2009).

Clearly, certain geothermal activities have the potential to produce seismicity that can be of public concern or even cause minor damage to infrastructure and buildings. For the future of geothermal energy in the Netherlands, it is therefore important to address the issue of induced seismicity in a proper way. A well-defined methodology is required for analysing induced seismicity risks prior and during geothermal project development. The methodology needs to fit into the legislation, needs to be supported by the industry, and needs to be accepted by the public.

The KennisAgenda Aardwarmte (Dutch Geothermal Research Agenda) has commissioned Q-con GmbH and its partner IF Technology B.V. to develop a protocol for induced seismicity in geothermal reservoirs in the Netherlands. The protocol is part of the knowledge data base (Kennisagenda) supporting geothermal project development in the Netherlands.

3 THEORETICAL ASPECTS OF INDUCED SEISMICITY

3.1 Physical Mechanisms

The phenomenon of man-made seismicity is known from different energy technologies such as mining, oil and gas exploitation, water impoundment and from geothermal reservoirs (National Research Council, 2012). The physical mechanisms underlying the induced seismicity are controlled by stress changes in the subsurface caused by anthropogenic activities.

If stress changes act on a pre-existing fracture or similar zone of weakness, seismicity may occur on the fracture if the shear stress exceeds the fracture strength. Let τ and σ_n denote the shear and normal stress resolved on a fracture plane, p_{fl} the *in situ* fluid pressure, μ the coefficient of friction and c_0 cohesion, then shear slippage occurs on the fracture if (e.g. Zoback, 2007):

Equation 1: $\tau > \mu \cdot (\sigma_n - P_{fl}) + c_{0.}$

Stress perturbations on a cohesionless fracture can be described by Coulomb stress changes *ΔCS*, which can be defined as (Scholz, 2002):

Equation 2: $\Delta CS = \Delta\tau - \mu \cdot (\Delta\sigma_n - \Delta p_{fl}),$

with $\Delta\tau$, $\Delta\sigma_n$, and Δp_{fl} denoting changes of shear-stress, normal-stress and fluid pressure, respectively. Positive *ΔCS* values increase the tendency to failure of a fracture.

The failure process of a fracture can be seismic or aseismic. For seismic failure, the fracture surfaces need to be mechanically strong enough to support high shear-stresses, and seismic energy is only released if the hardness of the fracture surfaces is sufficiently large to allow for an almost instantaneous failure. Sedimentary rocks usually exhibit a smaller strength compared to crystalline rock (e.g. Abdullah, 2006). This could explain why (noticeable) seismicity caused by geothermal operations typically occurs in basement rock (chapter 4).

Mechanisms causing seismicity in geothermal reservoirs according to Equation 2 include

- fluid pressure increase due to fluid injection,
- thermally induced stresses (thermal reservoir contraction),
- mass changes,
- poroelastic stress changes,
- and chemical processes.

All of these mechanisms may be relevant for a certain type of geothermal operation. It is noted, however, that the strongest seismic events observed to date in geothermal reservoirs (chapter 4) are interpreted as being caused by fluid overpressure.

3.2 Earthquake Strength

The strength of an induced event is primarily controlled by the dimension of the shearing plane associated with the event:

Equation 3: $M_0 = G \cdot A \cdot d,$

where M_0 is the seismic moment, G denotes shearing modulus, A is the area of the shearing plane, and d is the average slip occurring on the shearing plane.

The seismic moment can be determined from seismogram recordings assuming an earthquake model (e.g. Brune, 1970; Boatwright, 1980). Several empirical relationships exist to convert seismic moment to earthquake magnitude M_w. Most common is the definition by Hanks and Kanamori (1979)

Equation 4: $M_w = 2/3 \cdot log(M_0) - 6.1$

for which consistency with physical models has been demonstrated (Deichmann, 2006).

The moment magnitude scale as defined in Equation 4 is also used by KNMI (section 9.1), e.g. to determine earthquake strength of seismicity in the Groningen gas field. The standard magnitude scale used by KNMI, however, is a local magnitude M_L as defined in Dost et al. (2004), and later replaced (email comm. B. Dost, KNMI, 12.08.2013) by the M_L definition of Akkar et al. (2014). Equivalence of local and moment magnitude was generally assumed, i.e. $M_L \approx M_w$, but this assumption is currently being reviewed by KNMI.

For quantifying the strength of seismicity associated with geothermal operations in the Netherlands, the preferred magnitude scale is M_w according to Equation 4.

Figure 1 shows the relation between earthquake magnitudes and rupture length. When assuming a typical stress drop of 1 MPa, the rupture length of a magnitude 3.6 earthquake is approximately 1 km. A natural fault of this dimension is likely to be visible in a 3D seismic survey. Smaller (sub-seismic) faults, however, may still host relevant earthquakes.

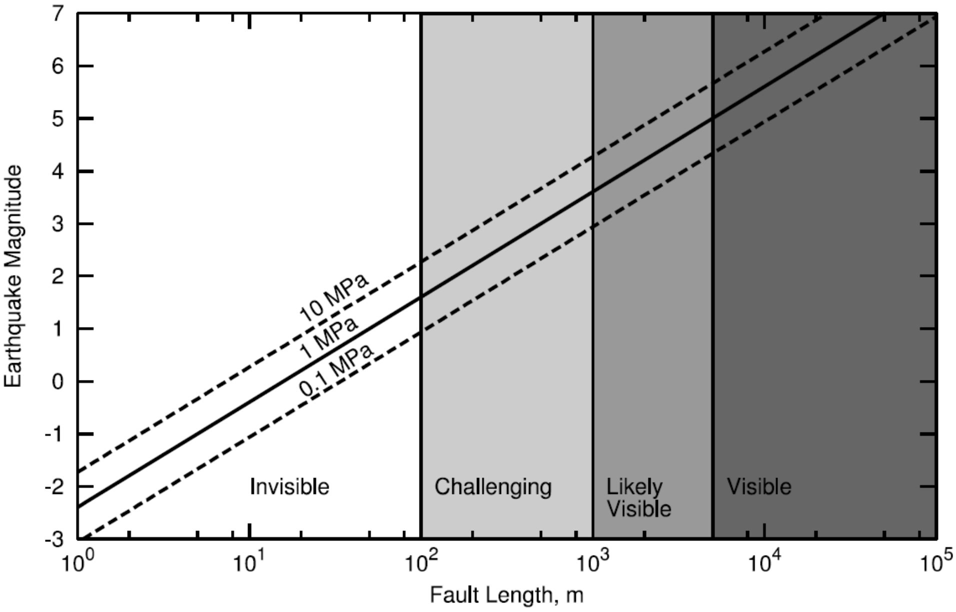

Figure 1: Theoretical relationship between fault rupture length (i.e. diameter of a circular fault patch), stress drop, and moment magnitude. Shaded regions denote "typical" visibility of a fault of a given length using three-dimensional (3-D) seismic survey. Source: White and Foxall (2014).

4 INDUCED SEISMICITY IN GEOTHERMAL SYSTEMS

4.1 Geothermal Exploitation Concepts in the Netherlands

Geothermal systems can be classified based on geological conditions and exploitation concept. Aside from volcanic regions, which are not relevant in the current context, it can be distinguished between hydrothermal and petrothermal systems. The latter are also referred to as Enhanced Geothermal Systems (EGS).

Hydrothermal systems are characterized by natural aquifers from which hot water can be (economically) produced. Petrothermal systems require artificial reservoir stimulation for producing water from an otherwise low permeable rock formation (typically basement rock). Frequently, induced seismicity is an essential factor for petrothermal reservoir stimulation since the deformations associated with induced seismicity result in a local enhancement of the hydraulic conductivity. Distinguishing between hydrothermal and petrothermal systems is not always straight forward and there exists a smooth transition between the two concepts.

Geothermal systems can be exploited by different configurations of production and re-injection wells.

The simplest system consists of a single production well (singlet). It requires a natural aquifer with sufficient fluid volume. This type of system is frequently used in balneology. For the Netherlands, singlet systems are not considered relevant.

Doublet, triplet, or multi-well systems consist of production and re-injection wells. At the surface, these systems are usually operated mass-balanced in a closed-loop. The concept of mass-balanced systems is considered most relevant for geothermal exploration in the Netherlands. Exploration concepts frequently involve aquifers in combination with a target fault zone, where a higher hydraulic conductivity is to be expected due to extensive fracturing.

4.2 Geothermal Project Data Base

In the following, the occurrence of induced seismicity associated with operational activities in hydrothermal and petrothermal reservoirs is summarized. Operations are categorised as stimulation, re-stimulation, and circulation.

The largest magnitude events are associated with hydraulic stimulations, where the driving mechanism for the seismicity is the hydraulic pressure increase in the subsurface (compare section 3.1). Hydraulic overpressures have also been identified as the cause for several seismic events that occurred during circulation operations under non-stationary hydraulic conditions in the subsurface (e.g. Landau, Germany in Table 1).

Table 1 lists projects that were identified as being relevant for the current study. The data base focusses on the Netherlands and neighboring countries, where geological conditions are comparable to local conditions in the Netherlands. Petrothermal (EGS) projects are included on a global scale.

The project list is inherently incomplete and the project selection is driven by availability of information rather than a completeness criterion. Especially smaller geothermal facilities that were never associated with induced seismicity may not show up in the scientific literature. This is different for projects associated with pronounced (felt) seismicity, where the project list is considered to be complete.

An important limitation of the data base is the project-specific lower detection threshold for induced seismicity. Many hydrothermal systems are operated without a local seismic monitoring system. It is therefore not straightforward to determine which system did or did not produce seismicity. Small magnitude earthquakes below the detection threshold of regional seismic monitoring networks may have occurred without being noticed. This is illustrated in Figure 2, where the typical lower detection threshold of a local monitoring station is almost two magnitude units lower than the detection threshold of a monitoring station located at 25 km distance.

Additionally, the detection threshold of the regional seismic monitoring networks is location- and time-dependent due to instrumental changes. The level of completeness common to all project regions considered here is perceptibility, i.e. all earthquakes strong enough to be felt by human beings are included in the regional catalogues. Except for Austria, however, the actual level of completeness is much lower for all project regions.

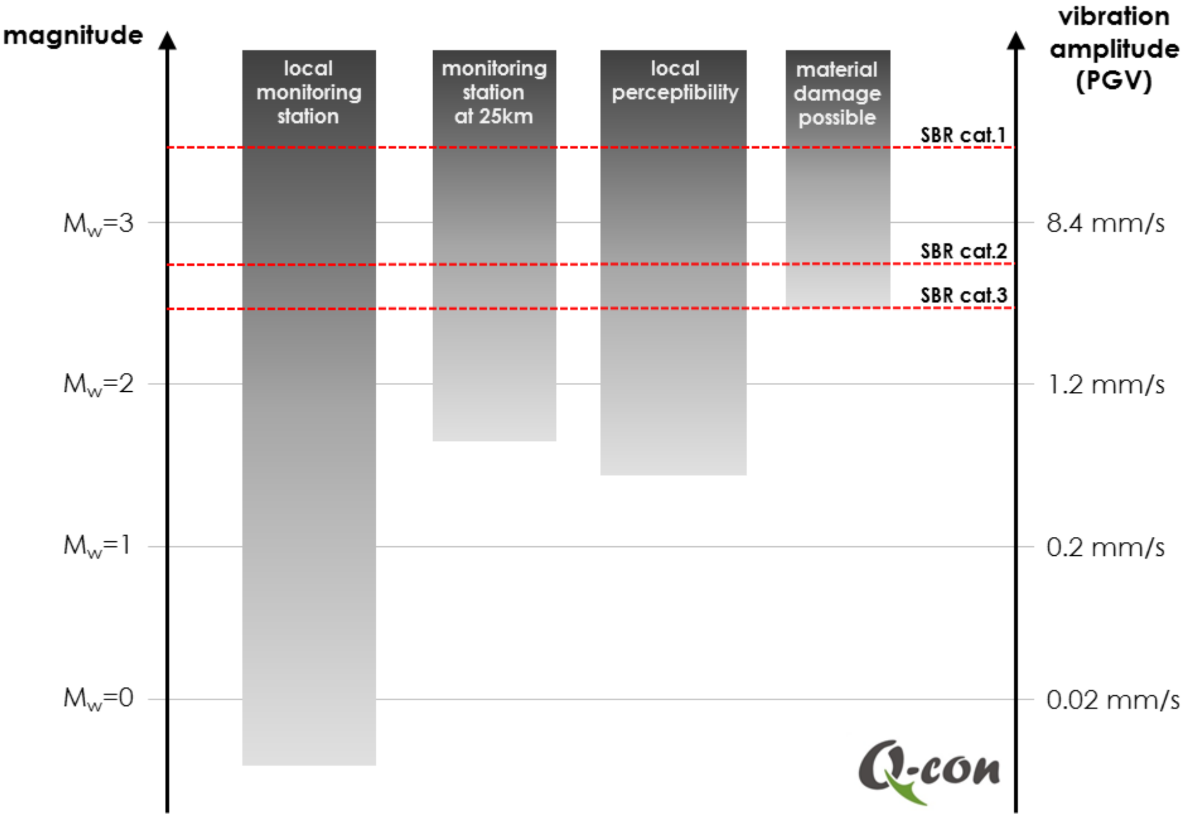

Figure 2: Sketch illustrating the relationship between earthquake magnitude and associated peak ground vibrations at the Earth's surface (PGV) for an earthquake located at 3 km depth. PGV values are based on the (mean) ground motion prediction equation of Douglas et al. (2013) in combination with near surface amplification factors as defined by Poggi et al. (2011) assuming a near surface shear wave velocity of V_{s30}=200 m/s and a dominating signal frequency of 10 Hz. Vibration levels above which damage is considered possible according to the SBR standard are indicated by dashed lines (cat 1: industrial buildings, cat 2: ordinary buildings, cat 3: sensitive buildings). The typical sensitivity range for a seismometer deployed in the epicenter and at 25 km distance, respectively, is indicated by shaded bars. Note the non-linear scale of the PGV axis.

Project	**Country**	**Type**	**Operation**	**LMS/TLS**	**M_{max}**	**Category**	**Rock type**
Bleiswijk - 1	Netherlands	hydrothermal	circ	No/No	-	sediment	sandstones (Cretaceous)
Bleiswijk - 1b	Netherlands	hydrothermal	circ	No/No	-	sediment	sandstones (Cretaceous)
Californië	Netherlands	hydrothermal	circ	Yes/Yes	M_L=0.3	sediment	carbonate (Carboniferous)
De Lier	Netherlands	hydrothermal	circ	No/No	-	sediment	sandstones (Cretaceous)
ECW	Netherlands	hydrothermal	circ	Yes/Yes	-	sediment	sandstones
Honselersdijk	Netherlands	hydrothermal	circ	No/No	-	sediment	sandstones (Jurassic/Cretaceous)
Koekoekspolder	Netherlands	hydrothermal	circ	No/No	-	sediment	sandstones (Permian)
Pijnacker (Ammerlaan)	Netherlands	hydrothermal	circ	No/No	-	sediment	sandstones (Cretaceous)
Pijnacker (Duijvestijn)	Netherlands	hydrothermal	circ	No/No	-	sediment	sandstones (Cretaceous)
Vierpolders	Netherlands	hydrothermal	circ	No/No	-	sediment	sandstones
Aschheim	Germany	hydrothermal	circ	?/?	-	sediment	carbonate (Malm)
Bad Urach 2002	Germany	EGS	stim	Yes/Yes	M_L=1.8	basement	gneiss (metamorphic)
Bad Urach 2003	Germany	EGS	re-stim	Yes/Yes	M_L=1.4	basement	gneiss (metamorphic)
Bruchsal	Germany	hydrothermal	circ	Yes/No	-	sediment	sandstone
Brühl	Germany	hydrothermal /EGS	stim	Yes/Yes	-	sediment	sandstones (Middle Buntsandstein)
Dürrnhaar	Germany	hydrothermal	circ	?/?	-	sediment	carbonate (Malm)
Erding	Germany	hydrothermal	circ	?/No	-	sediment	carbonate (Malm)

Project	Country	Type	Operation	LMS/TLS	M_{max}	Category	Rock type
Garching	Germany	hydrothermal	circ	?/?	-	sediment	carbonate (Malm)
Groß Schönebeck	Germany	EGS	stim	Yes/Yes	M_L= -1.1	vulcanite	volcanics - sandstones (Lower & Upper Rotliegend)
Hannover (GeneSys)	Germany	EGS	stim	Yes/Yes	-	sediment	sandstone (Middle Buntsandstein)
Horstberg (GeneSys)	Germany	EGS	stim	Yes/Yes	-	sediment	sandstone (Middle Buntsandstein)
Insheim (GTI-1)	Germany	hydrothermal /EGS	stim	Yes/Yes	M_L=2.4	basement - sediment	granite - sandstone -carbonate
Ismaning	Germany	hydrothermal	circ	Yes/?	-	sediment	carbonate (Malm)
Kirchstockach	Germany	hydrothermal	circ	Yes/No	M_L= 0.5	sediment	carbonate (Malm)
Kirchweidach	Germany	hydrothermal	circ	Yes/No	-	sediment	carbonate (Malm)
KTB - 1994	Germany	research	stim	Yes/No	M_L=1.2	basement	gneiss
KTB - 2000	Germany	research	stim	Yes/No	M_L=0.7	basement	gneiss
Landau in der Pfalz	Germany	hydrothermal /EGS	circ	Yes/Yes	M_L=2.7	basement - sediment	granite – sandstone - carbonate
München Riem	Germany	hydrothermal	circ	?/?	-	sediment	carbonate (Malm)
Neubrandenburg	Germany	hydrothermal	circ	No/No	-	sediment	sandstone
Neustadt-Glewe	Germany	hydrothermal	circ	No/No	-	sediment	sandstone
Oberhaching (Grünwald)	Germany	hydrothermal	circ	?/?	-	sediment	carbonate (Malm)
Poing	Germany	hydrothermal	circ	?/?	-	sediment	carbonate (Malm)
Pullach	Germany	hydrothermal	circ	?/?	-	sediment	carbonate (Malm)
Sauerlach	Germany	hydrothermal	circ	Yes/?	-	sediment	carbonate (Malm)

Project	Country	Type	Operation	LMS/TLS	M_{max}	Category	Rock type
Simbach-Braunau	Germany	hydrothermal	circ	No/No	-	sediment	carbonate (Malm)
Taufkirchen	Germany	hydrothermal	circ	Yes/No	M_L= 0.3	sediment	carbonate (Malm)
Traunreut	Germany	hydrothermal	circ	Yes/Yes	-	sediment	carbonate (Malm)
Unterföhring	Germany	hydrothermal	circ	?/?	-	sediment	carbonate (Malm)
Unterföhring II	Germany	hydrothermal	circ	?/?	-	sediment	carbonate (Malm)
Unterhaching	Germany	hydrothermal	circ	Yes/No	M_L=2.4	sediment	carbonate (Malm)
Unterschleißheim	Germany	hydrothermal	circ	Yes/?	-	sediment	carbonate (Malm)
Waldkraiburg	Germany	hydrothermal	circ	?/?	-	sediment	carbonate (Malm)
DHM Basel	Switzerland	EGS	stim	Yes/Yes	M_L=3.4	basement	granite
Riehen	Switzerland	hydrothermal	circ	No/No	-	sediment	carbonate (Trias - Muschelkalk)
St. Gallen	Switzerland	hydrothermal	stim	Yes/Yes	M_L=3.5	sediment	carbonate (Malm)
Altheim	Austria	hydrothermal	circ	No/No	-	sediment	carbonate (Malm)
Bad Blumau	Austria	hydrothermal	circ	No/No	-	sediment	Devonian carbonate, karstified or fractured
Geinberg	Austria	hydrothermal	circ	No/No	-	sediment	carbonate (Malm)
Obernberg	Austria	hydrothermal	circ	No/No	-	sediment	carbonate (Malm)
Mehrnbach	Austria	hydrothermal	circ	No/No	M_L=1.8	sediment	carbonate (Malm)
St. Martin i. Innk.	Austria	hydrothermal	circ	No/No	-	sediment	carbonate (Malm)
Paris Basin (multiple projects)	France	hydrothermal	circ	No/No	-	sediment	carbonate (Dogger)

Project	Country	Type	Operation	LMS/TLS	M_{max}	Category	Rock type
Rittershofen GRt1	France	hydrothermal /EGS	stim	Yes/?	M_L=1,5	basement - sediment	granite - buntsandstein
Soultz-sous-Forêts (GPK1 – 1993)	France	EGS	stim	Yes/No	M_L=1,9	basement	granite
Soultz-sous-Forêts (GPK1 – 1993)	France	EGS	re-stim	Yes/No	M_L=1,6	basement	granite
Soultz-sous-Forêts (GPK1, GPK2 – 1997)	France	EGS	circ	Yes/No	-	basement	granite
Soultz-sous-Forêts – (GPK2 – 2000)	France	EGS	stim	Yes/No	M_L=2.6	basement	granite
Soultz-sous-Forêts (GPK3 – 2003)	France	EGS	stim	Yes/No	M_L=2.9	basement	granite
Soultz-sous-Forêts (GPK4 – 2004)	France	EGS	stim	Yes/No	M_L=2.3	basement	granite
Soultz-sous-Forêts (GPK4 – 2005)	France	EGS	re-stim	Yes/No	M_L=2.7	basement	granite
Soultz-sous-Forêts (GPK1,2,3 - 2010)	France	EGS	circ	Yes/No	M_L=2.3	basement	granite
Rosemanowes	UK	EGS / research	circ	Yes/No	ML=2.0	basement	granite
Fjällbacka	Sweden	EGS / research	stim	Yes/?	M_L= -0.2	basement	granite
Cooper Basin (H#1) 2003	Australia	EGS	stim	Yes/Yes	M_L=3.7	basement	granite
Cooper Basin (H#1) 2005	Australia	EGS	re-stim	Yes/Yes	M_L=2.9	basement	granite
Cooper Basin (H#2) 2005	Australia	EGS	stim	Yes/Yes	M_L=2.6	basement	granite
Cooper Basin (H#3) 2008	Australia	EGS	stim	Yes/Yes	M_L=1.7	basement	granite
Cooper Basin (J#1) 2010	Australia	EGS	stim	Yes/Yes	M_L=1.6	basement	granite

Project	Country	Type	Operation	LMS/TLS	M_{max}	Category	Rock type
Cooper Basin (H#4) 2012	Australia	EGS	stim	Yes/Yes	M_L=3.0	basement	granite
Paralana	Australia	EGS	stim	Yes/Yes	M_L=2.6	basement - sediment	mesoproterozoic felsic porphyry - sediment
Hijiori	Japan	EGS / research	stim	Yes/?	M=0.3	basement	granodiorite
Ogachi	Japan	EGS / research	stim	Yes/?	M_L=2.0	basement	granodiorite
Fenton Hill	USA	EGS / research	stim	Yes/No	M_w=1.3	basement	granitic rock
Newberry, Oregon	USA	EGS	stim	Yes/Yes	M_L=2.3	vulcanite	basalt flows - dikes - granodiorite intrusive

Table 1: Overview of hydrothermal and petrothermal (EGS) projects. Operations are categorized as stimulation (stim), re-stimulation (re-stim), and circulation (circ). LMS and TLS indicate whether or not a local seismic monitoring station or a traffic-light system (compare chapter 10) were operated. M_{max} denotes the maximum seismic event magnitude associated with the project (dash indicates no seismicity). Missing information is marked by question marks.

4.3 Spatio-Temporal Evolution and Earthquake Strength

Seismicity induced in geothermal reservoirs typically exhibits a distinct spatio-temporal pattern, where the seismic activity successively migrates away from an injection point, consistent with the propagation of a hydraulic pressure front (e.g. Shapiro et al., 1997).

Observations made during various hydraulic stimulations indicate that seismicity occurs only at those locations, where the previously experienced *in situ* fluid pressure is exceeded. This is the so called Kaiser-Effect, which follows directly from the Mohr-Coulomb failure criterion (Baisch and Harjes, 2003). The same phenomenon has also been referred to as a ‘back front’ of the induced seismicity (Parotidis et al., 2004). Examples of the systematic spatio-temporal evolution of seismicity during hydraulic stimulation are shown in Figure 3.

Consistent with the temporal growths of the pressurized subsurface volume, maximum event magnitudes systematically increase during hydraulic stimulation operations (Figure 4). This characteristic behavior provides the basis for implementing a 'Traffic Light System' for risk mitigation (chapter 10).

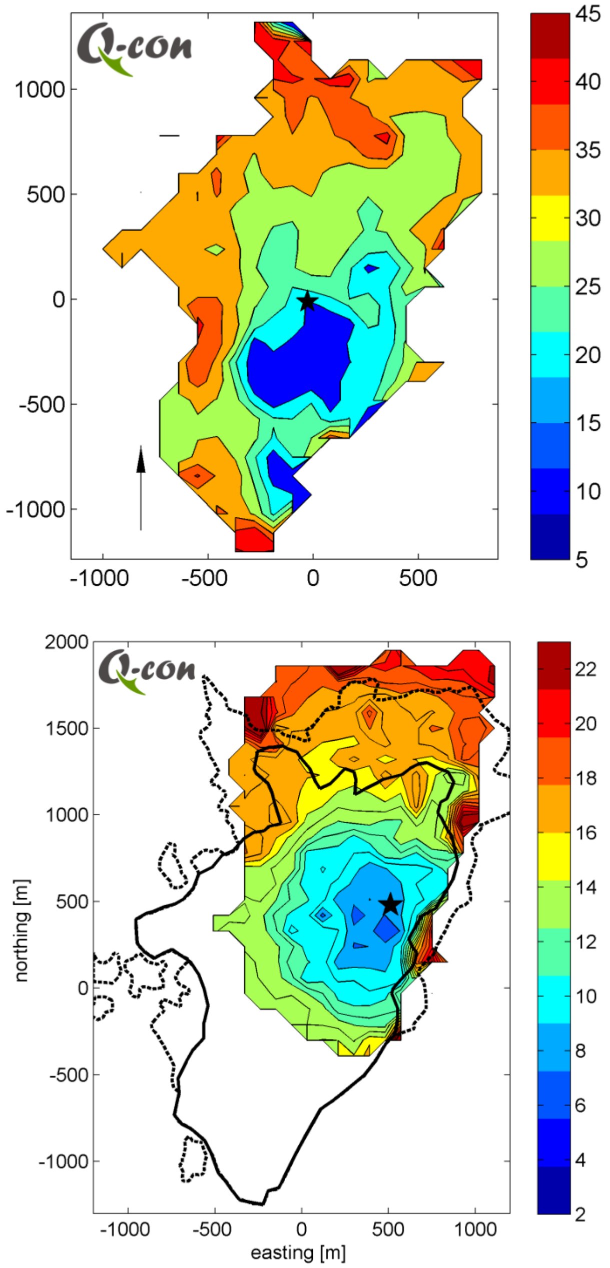

Figure 3: Spatiotemporal distribution of the seismic activity during hydraulic stimulations in the Cooper Basin (Australia) in map view. Seismic activity is restricted to a narrow sub-horizontal layer structure. Averaged occurrence times (in days with respect to the beginning of the stimulation) are displayed by contours according to the colormap. Star denotes the location of the injection well. Note the systematic spatio-temporal evolution of the seismicity comprising several ten thousand events. Figures reproduced from Baisch et al. (2006; 2015).

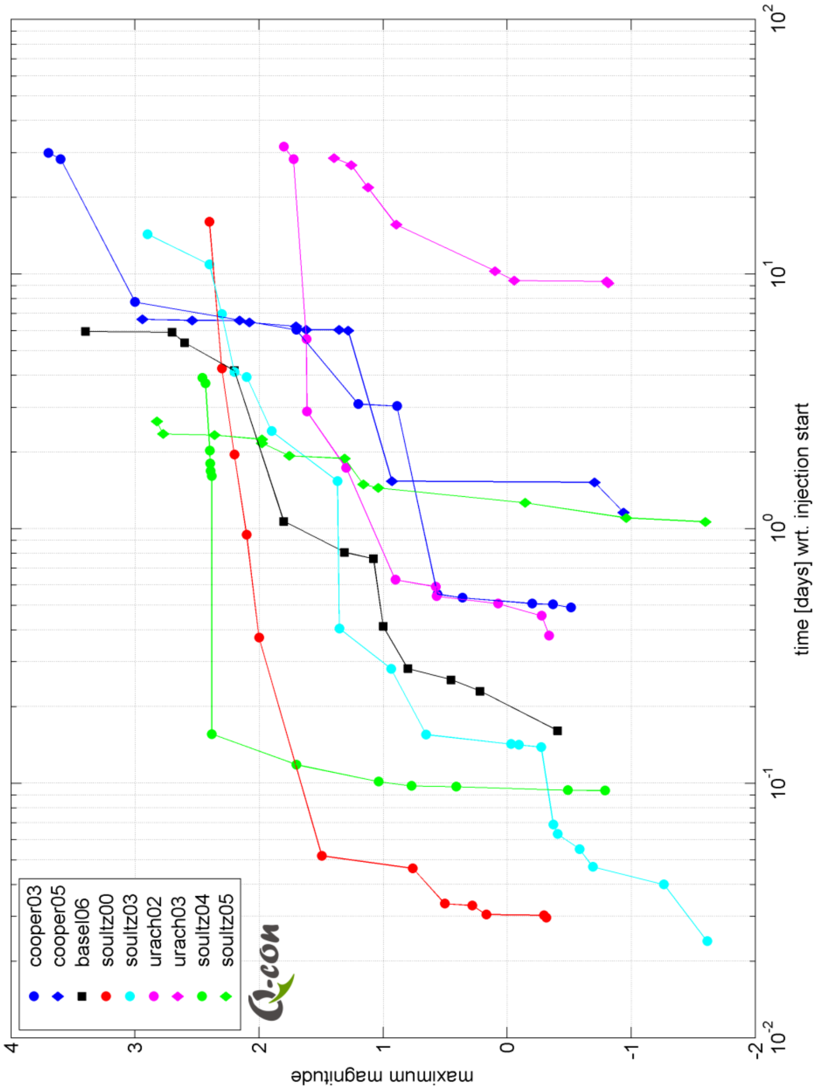

Figure 4: Maximum event magnitude as a function of injection time during hydraulic stimulation at different geothermal sites. Multiple stimulations of a well are indicated by using the same color and diamond symbols for indicating re-stimulation. Note that data points are generated whenever previous maximum magnitudes are exceeded. Thus, a large number of data points indicate a gradual increase of the maximum event magnitude. Figure taken from Baisch et al. (2009).

4.4 Post-Operational Seismicity

In the previous section, it was shown that the strength of induced seismicity systematically increases with time during fluid injections. Frequently, seismicity does not stop immediately after an injection operation[1] is terminated (see example in Figure 5). This can be explained by an ongoing fluid pressure diffusion process causing post-injection seismicity (Baisch et al., 2006b). Accordingly, the trend of increasing event magnitudes often continues in the post-injection period (Figure 6). For operating a traffic-light-system (chapter 10), this ‘trailing effect’ (i.e. the post-operational magnitude increase) is a major challenge, especially since operational mitigation matters are limited (operations stopped already). Therefore, the magnitude of the trailing effect has to be anticipated when designing a traffic-light-system.

The magnitude of the trailing effect is depending on details of the local hydro-geological conditions, as well as on the operations. A large volume injection into a low-permeable formation is more prone to a trailing effect than a similar injection into a highly conductive aquifer. Systems operated under quasi-stationary hydraulic conditions in the subsurface do not produce trailing effects based on pressure diffusion. The largest trailing effect to date was observed after the stimulation of the DHM geothermal reservoir at Basel (Switzerland). Here, a post-injection magnitude increase of 0.5 magnitude units (M_w) was observed. Examples of post injection seismicity in different EGS projects are shown in Figure 6.

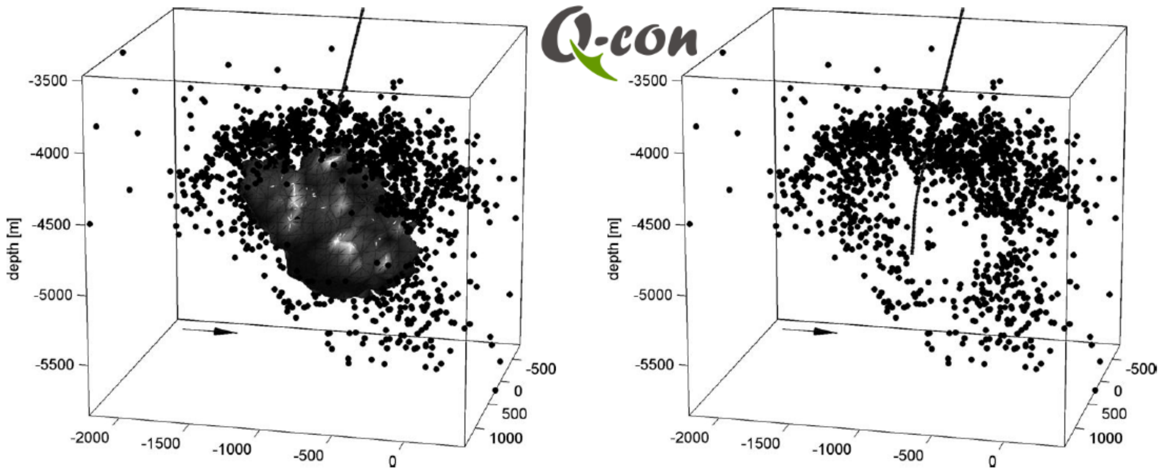

Figure 5: Comparison between the seismic activity induced during the 2003 Soultz-sous-Forêts (France) hydraulic stimulation and the post-injection seismicity. Stimulation seismicity is shown by an isosurface of the hypocenter density (left). Post-injection seismicity (dots) occurs exclusively at the outer rim of the previously stimulated zone. Solid line denotes injection well. Figure taken from Baisch et al. (2006b).

[1] this applies also to geothermal production operations where fluid is re-injected into the subsurface

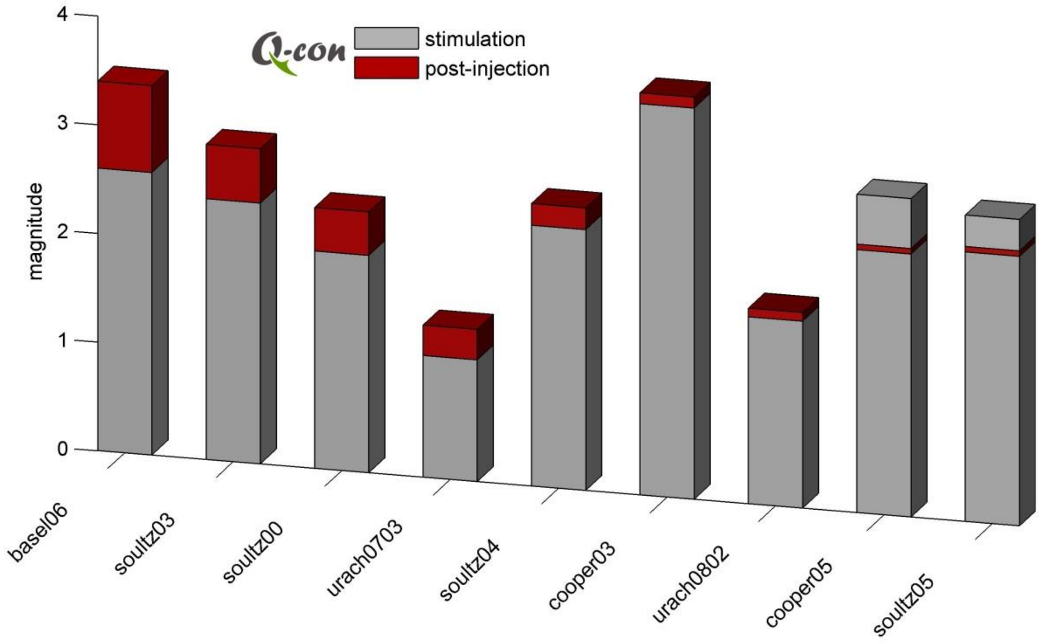

Figure 6: Observed event magnitudes during hydraulic stimulation (grey) and during the post-injection period (red) at selected geothermal sites listed in Table 1. The data have been sorted according to the difference between injection and post-injection magnitudes. The largest difference is observed at the geothermal reservoir at Basel (Switzerland), where the post-injection magnitude exceeds previous event magnitudes by 0.8 units (M_L) corresponding to 0.5 units (M_w). In two projects ('cooper05' and 'soultz05'), the largest magnitude event occurred already during stimulation. Figure is taken from Baisch et al. (2009).

5 DEFINITION OF KEY PARAMETERS

From the previous discussion it is evident that the occurrence of induced seismicity requires a specific combination of different subsurface conditions. Hence, the strength of induced seismicity is not controlled by a single parameter only.

It is nevertheless likely that seismicity strength scales with certain parameters if – at the same time - other parameters meet the requirements for seismic failure. In the following sections, the most relevant parameters are defined.

5.1 Geological Parameters

5.1.1 Hydraulic connection to crystalline basement

Various studies indicate that the crystalline crust commonly is in a critical stress state, where only minor stress perturbations are sufficient to induce seismicity (e.g. Townend and Zoback, 2000). Accordingly, direct fluid injection into the crystalline rock typically produces seismicity. Evans et al. (2011) notice that the largest magnitude seismic events associated with geothermal activities in Europe consistently occurred in basement rock. Their data base supports the view that sedimentary rocks tend to be less seismogenic than crystalline rocks.

In the Netherlands, the depth of the crystalline basement is not well constrained. In Figure 7 the depth level of the pre-Silesian is shown. Below this level a significant thickness of Devonian sediments is likely to be present. For most parts of the Netherlands it can therefore be concluded that the crystalline basement is located significantly deeper than today's geothermal target depth. A direct hydraulic connection to the crystalline basement can in principle be established through permeable faults running from the geothermal reservoir level into the basement. In a low permeable rock environment, hydraulic overpressure can be transmitted over a considerable distance along a fault with the potential to trigger seismicity at several kilometres distance (e.g. National Research Council, 2012).

Although a seismicity response to overpressures cannot be excluded in the rock formations overlying the crystalline basement, direct hydraulic connection to the crystalline basement is considered most relevant for the seismic hazard.

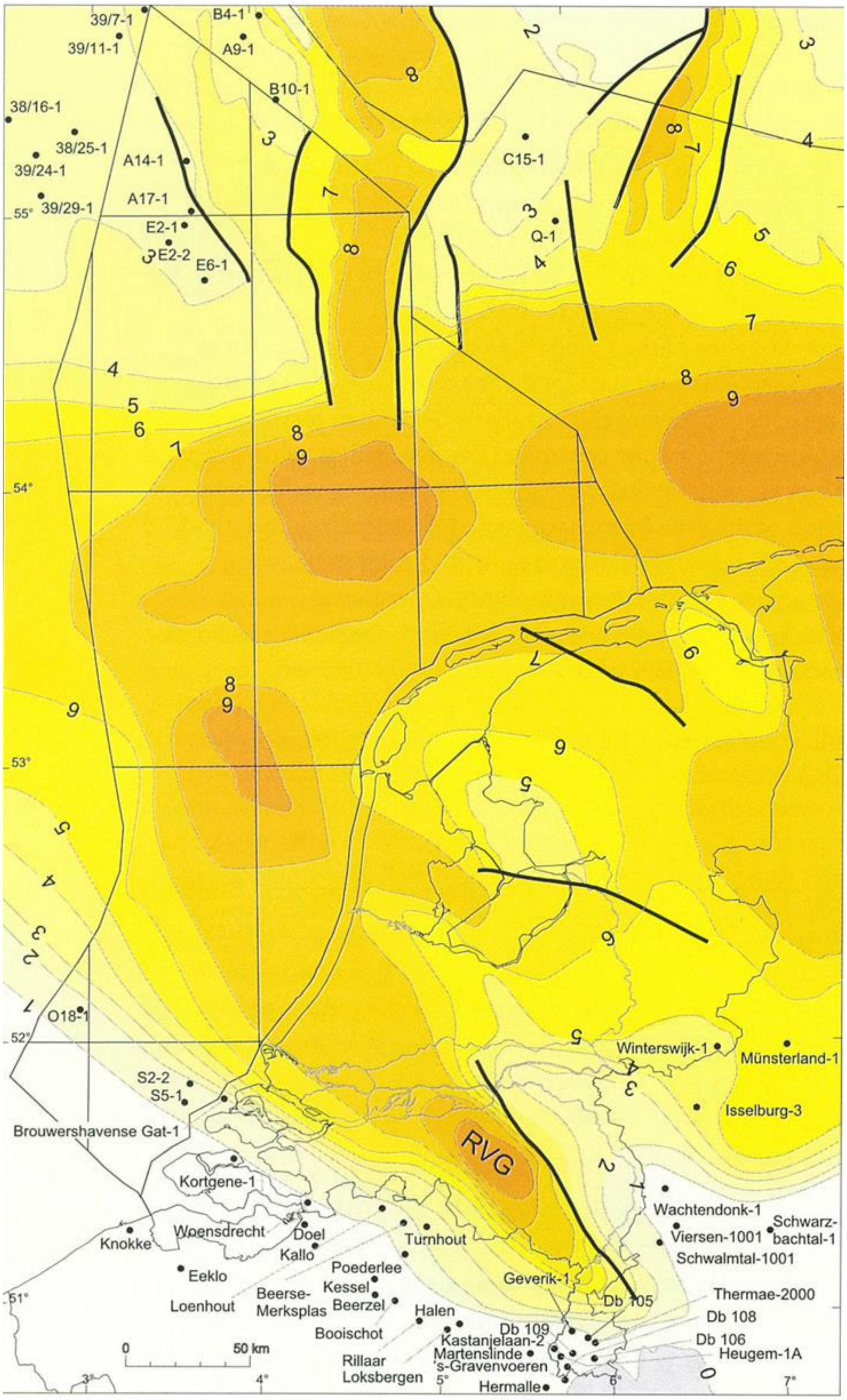

Figure 7: Schematic depth map in kilometres of the top of the pre-Silesian. Wells which encountered the pre-Silesian are indicated. Figure from Geluk et al. (2007).

5.1.2 Distance to natural faults

From the previous discussion it is evident that critically stressed faults play a decisive role for the seismic hazard. In particular larger scale faults (e.g. lateral fault extension >1 km) have the potential to host damaging earthquakes.

Identifying critically stressed faults near a future geothermal reservoir, however, has practical limitations. Even a 3D seismic survey will not necessarily detect all faults of a size that is relevant for the seismic hazard (Figure 1). On the other hand, faults are abundant over the whole of the Netherlands (see example in Figure 8) and most faults resolved in a seismic survey will not be critically stressed. Besides the size of a fault it is therefore important to consider the regional tectonic context and the fault orientation in the current stress field (compare section 5.1.3).

Identifying potentially relevant faults prior to geothermal project development is inherently uncertain. Fault traces are subject to location uncertainty and the distance over which geothermal activities can cause seismicity is depending on details of the stress- and strength-conditions on the fault.

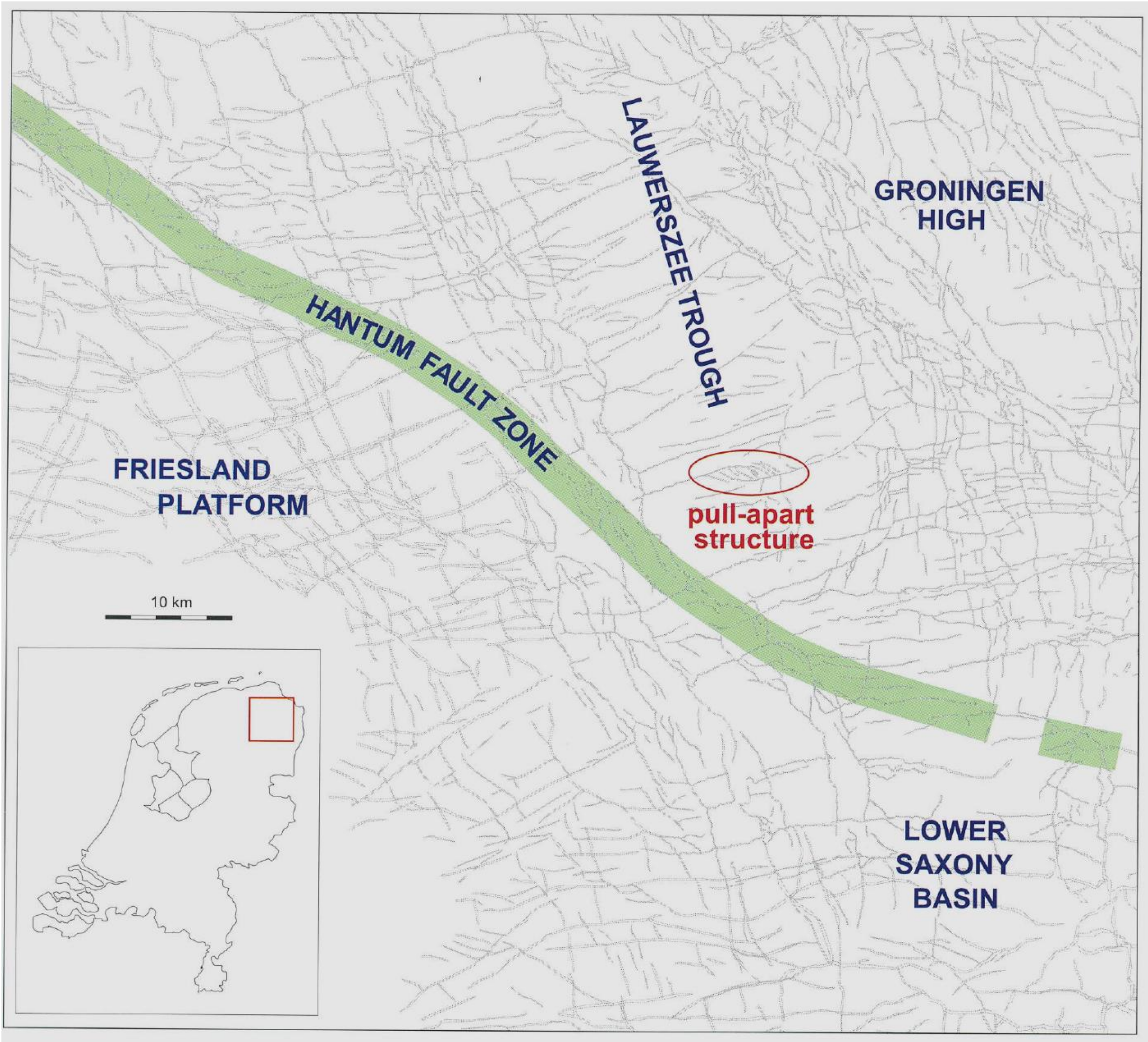

Figure 8: Fault pattern at Roliegend level, north-east Netherlands. Figure from De Jager (2007).

5.1.3 Orientation of natural faults in current stress field

The stability of a fault is depending on the stresses acting on the fault as well as on the strength of the fault (Equation 1). Tectonic stresses acting on a fault are determined by the orientation of the fault with respect to the tectonic stress field. Some faults are effectively locked in the current stress field and other faults are oriented more favourably for failure. For a given fault trajectory, this can be assessed using models of the local or regional stress field (e.g. Heidbach et al., 2009). The fault strength (i.e. coefficient of friction and cohesion), however, is uncertain and cannot be assessed by existing geophysical exploration technologies. For hazard and risk evaluations based on geomechanical models, assumptions have to be made regarding the possible range of fault strength. For the Quick Scan, however, the orientation of a fault serves only as a proxy for stress criticality.

5.2 System Parameters

In the following sections, correlations between earthquake magnitude and operational parameters are shown. The underlying data base contains the projects listed in Table 1. Some of the project data is not released to the public and can only be presented in abstracted form, without making reference to the specific project.

5.2.1 Net injected fluid volume

Based on theory, injected fluid volume has been identified to be a relevant parameter controlling the strength of induced earthquakes (McGarr, 1976; 2014). McGarr's theoretical concept addresses unbalanced injections such as hydraulic reservoir stimulation.

Figure 9 shows maximum earthquake magnitude as a function of injected volume for geothermal reservoir stimulations. The maximum earthquake magnitude tends to increase with the net injected volume. In absence of critically stressed faults, however, some large volume fluid injections did not induce any measurable seismicity (e.g. Horstberg/Germany in Table 1), demonstrating that the seismicity response depends on parameter combinations rather than on a single parameter.

For geothermal circulation, the net injected volume can be defined as the difference between injected and produced fluid volume. This definition implies negligible net injected volume when the system is operated in mass-balanced mode at surface (i.e. produced volume equals re-injected volume).

It is emphasized, however, that the net injected volume as defined here is not an appropriate proxy for the seismic hazard if production and injection wells exhibit poor hydraulic connection at reservoir level. To account for this, 'inter-well pressure communication' and 'circulation rate' are included as additional key parameters.

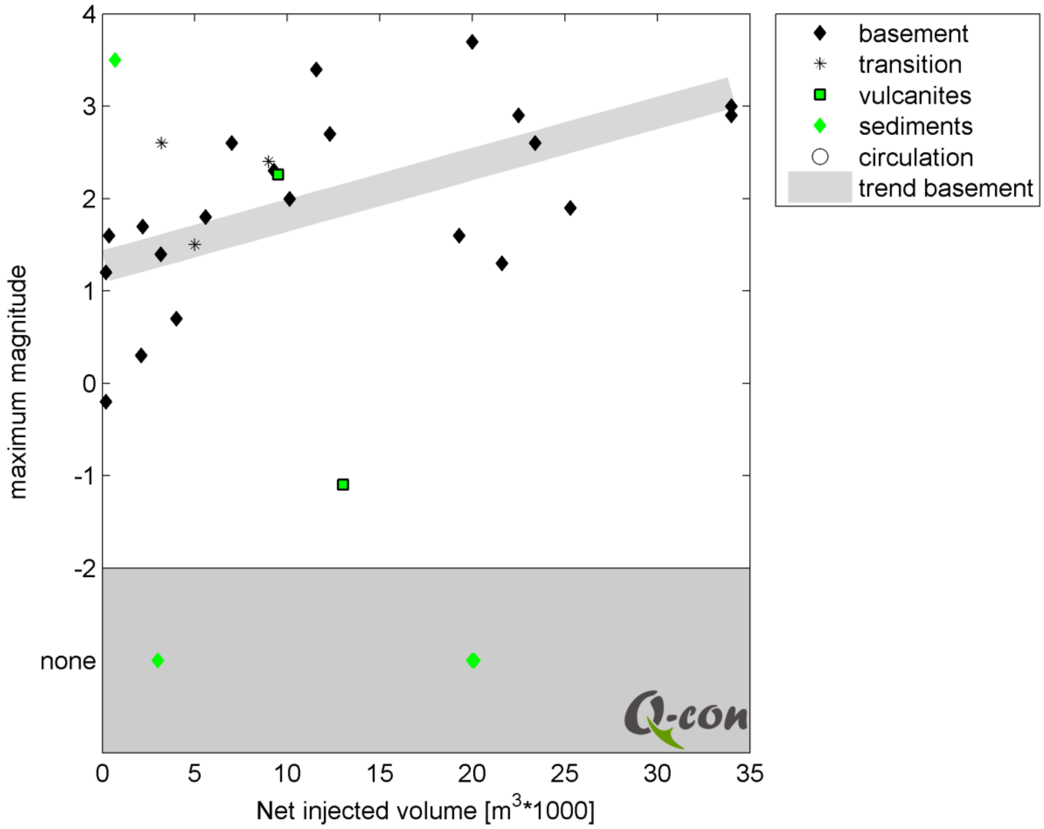

Figure 9: Maximum magnitude of induced events as a function of the (net) injected volume for projects listed in Table 1. Rock type of the target formation is indicated according to the legend. Trend line was fitted to basement data points (light grey). Data points with no seismicity were discarded for fitting trend line.

5.2.2 Inter-well pressure communication

As outlined in the previous section, hydraulic communication between the injection and production wells at reservoir level is an important aspect for the seismic hazard. Currently, all deep geothermal systems in the Netherlands are operated mass balanced at the surface, i.e. the net injected volume is zero.

Relevant for the seismic hazard, however, is the mass balance in the subsurface. In the extreme case, where the re-injection well is hydraulically isolated from the production well by sealing barriers in the subsurface, geothermal circulation implies a continuous, large volume hydraulic stimulation.

From a seismic hazard perspective, this scenario has to be avoided. On the other hand, direct hydraulic connection between injection and production wells bears the risk of a premature thermal breakthrough. Finding a reasonable balance between these counteracting aspects is an important task of the geothermal system design.

In a typical configuration, production and injection wells are drilled to a similar depth into the same reservoir formation and are separated by 1-2 km at reservoir level. If the reservoir exhibits good hydraulic transmissivity and if there are no sealing barriers in between the two wells, this configuration reflects a reasonable compromise.

5.2.3 (Re-)Injection pressure

As a necessary condition for the occurrence of fluid injection induced seismicity, the *in situ* fluid pressure on a seismogenic fault has to exceed a critical level (Equation 1). In principle, the re-injection pressure controls the level of overpressure in the reservoir formation. The injection pressure level at which seismicity can be induced, however, is depending on details of the seismogenic fault and a number of other parameters such as hydraulic friction losses, and the duration time over which overpressures are applied.

Figure 10 shows maximum earthquake magnitude as a function of the (re-)injection pressure for geothermal reservoir stimulation and circulation operations. A correlation between these two parameters is not obvious, which could simply reflect the importance of the additional parameters discussed above.

Observation data in Figure 10 cover a large range of injection pressure, from almost zero up to 70 MPa. This is much larger than estimates of the fluid overpressure required to induce seismicity. For example, induced seismicity in the Soultz-sous-Forêts geothermal reservoir starts at overpressures of 3 MPa (Baria et al., 2004). Much smaller values of the triggering pressure are discussed in the scientific literature (see summary report of Costain and Bollinger, 2010).

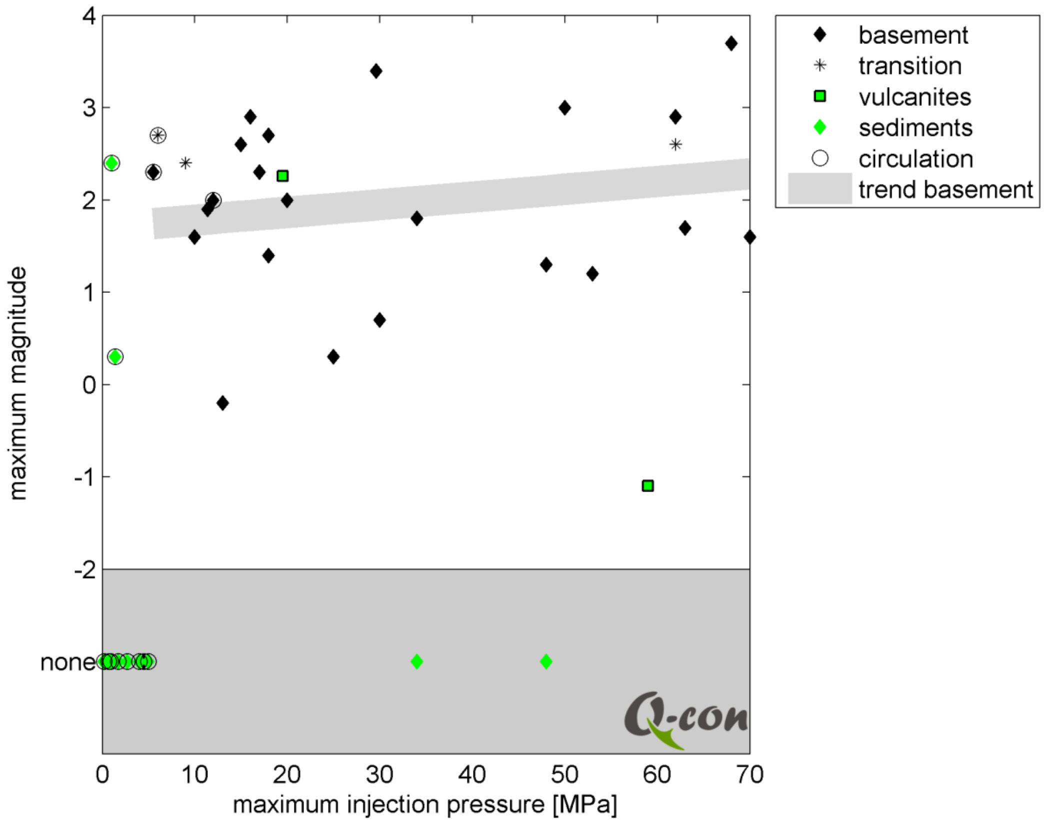

Figure 10: Maximum magnitude of induced events as a function of the (re-)injection pressure for projects listed in Table 1. Rock type of the target formation is indicated according to the legend. Symbols in circles denote circulation operations, open symbols denote fluid injection. Trend line was fitted to basement data points (light grey). Data points with no seismicity were discarded for fitting trend line.

5.2.4 Circulation Rate

In the previous section, injection pressure was identified as a key parameter for the seismic hazard. Injection pressure is the system response to the injection rate. At first glance, circulation rate does therefore not appear to be a key parameter.

For a scenario, where injection and production well are hydraulically isolated at reservoir level, it was noted that the relevant injection volume will be grossly underestimated when considering the net injected volume (section 5.2.1). In this case, the circulation rate provides another means for addressing the unbalanced fluid volume injected into the reservoir. Therefore, circulation rate is considered an additional key parameter.

Figure 11 shows maximum earthquake magnitude as a function of injection rate for geothermal reservoir stimulation and circulation operations. A correlation between these two parameters is not obvious, although a slight trend of increasing magnitude with circulation rate exists.

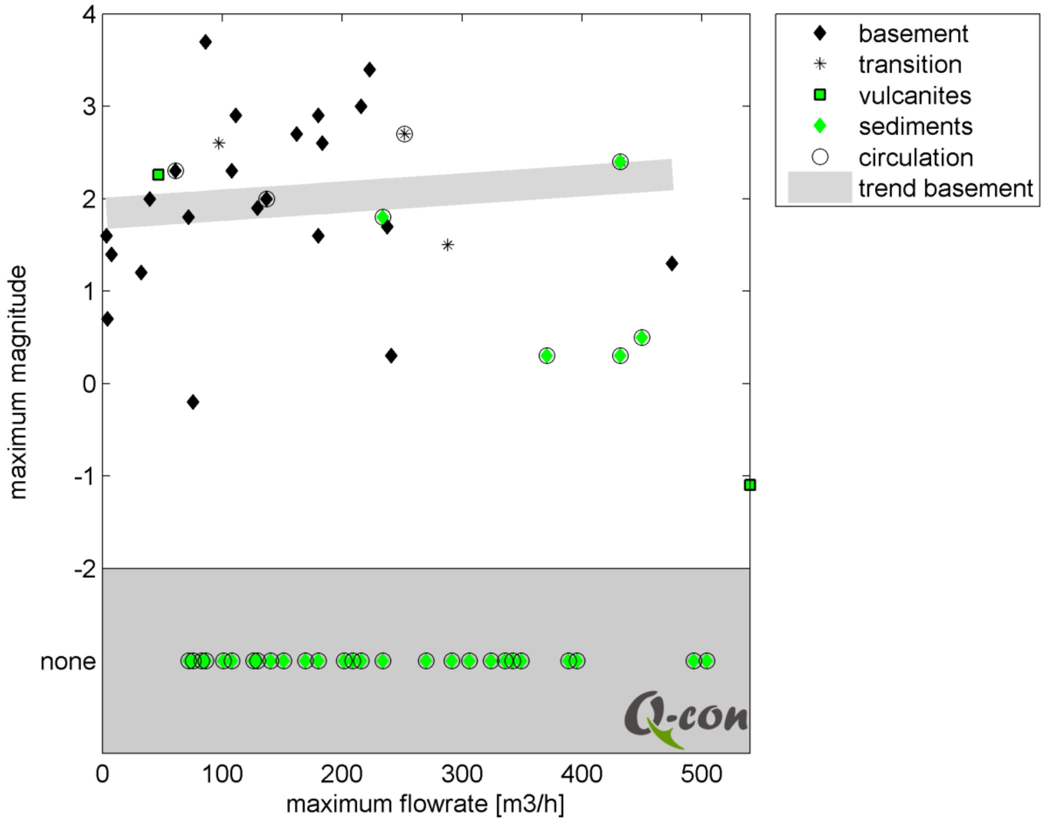

Figure 11: Maximum magnitude of induced events as a function of the (re-)injection rate for projects listed in Table 1. Rock type of the target formation is indicated according to the legend. Symbols in circles denote circulation operations, open symbols denote fluid injection. Trend line was fitted to basement data points (light grey). Data points with no seismicity were discarded for fitting trend line.

5.2.5 Parameters Not Considered

5.2.5.1 Pressure decrease

Experience from a large number of gas fields in the Netherlands demonstrates that decreasing the reservoir pressure by gas production can cause seismicity (e.g. Mulders, 2003; van Wees et al., 2015). According to Equation 1, this may appear counterintuitive since pressure decrease increases the effective normal stress on reservoir faults thus stabilizing them. At large pressure depletion levels, however, reservoir compaction becomes a dominating effect. Under certain conditions, reservoir compaction can increase differential stresses on reservoir faults (known as differential compaction, e.g. Bourne and Oates, 2015), which are larger than the stabilizing effect of the hydraulic pressure decrease.

Observation data from more than 190 gas fields in the Netherlands indicate that compaction driven seismicity occurs only if the reservoir is depleted by more than 110 bar (van Eijs et al., 2006) or by more than 28% of the initial reservoir pressure (Van Thienen-Visser et al., 2012). It should be noted that depletion in gas reservoirs typically refers to a larger scale process, frequently with a field-wide dimension.

During geothermal circulation, the reservoir pressure is lowered at the production wells e.g. by a production pump. The typical pressure decrease in a geothermal production well is much smaller than 110 bar due to technical and/or regulating limitations. Furthermore, the pressure decrease is a localized process centered at the production well(s) due to the higher viscosity of water compared to gas.

Therefore, pressure decrease and the associated differential compaction is not considered relevant for the seismic hazard in geothermal systems.

5.2.5.2 Thermal Reservoir Compaction

Significant thermal stress changes occur in the immediate vicinity of an injection well (e.g. Ghassemi et al., 2008; Segall and Fitzgerald, 1998), which may lead to a process referred to as ‘thermal fracking’. Due to its localized nature, however, this process is not considered relevant in the context of seismic hazard.

A significant amount of heat is withdrawn from the subsurface over the lifetime of a geothermal system. Reservoir cooling starts at the injection well(s) and systematically propagates outwards with time, while the cooling pattern is determined by the dominating flow paths. The associated thermal compaction of the reservoir rock causes stress changes, which theoretically could induce seismicity on a nearby fault. Although this effect has been studied numerically (e.g. Baisch et al., 2009), no observation data exists where induced seismicity could be unambiguously attributed to this effect.

Therefore, reservoir cooling is not included as a Quick-Scan parameter (section 8.1), but it is recommended to address thermal reservoir compaction as part of a Level 2 (section 8.2) and a Level 3 (section 8.3) assessment.

5.3 Previous Seismicity

The occurrence of natural seismicity near a geothermal site demonstrates the existence of natural, seismically active fault zones. In such an environment, an increased seismic hazard results when operating a geothermal system as seismicity might already be caused[2] by relatively small stress perturbations.

Proximity to (potentially) active faults is considered a key parameter in the context of seismic hazard. Due to their large dimension, natural faults may host significant earthquakes. For example, faults with a dimension in the order of 1 km^2 may host M_w=4 earthquakes.

The critical distance over which stress perturbations associated with geothermal operations may cause seismicity on a natural fault is depending on details of the fault, in particular on

[2] In the scientific literature, the terminology ‘triggered earthquake’ is sometimes used for earthquakes initiated by anthropogenic operations, but where the earthquake process is driven by tectonic stresses. Accordingly, the terminology ‘induced earthquake’ is applied to earthquakes where the driving stresses are predominantly caused by the anthropogenic activities. A clear separation of these two scenarios is often not possible. In the current study, the terminologies ‘induced’, ‘triggered’, and ‘caused’ are therefore used interchangeably.

actual stress/strength conditions and the fault geometry. Theoretically, the stress-state on a natural fault can get arbitrarily close to failure during the nucleation process of a tectonic earthquake, and minor stress perturbations may already be sufficient to initiate the earthquake. This scenario is considered relevant in tectonically active areas.

For the Quick-Scan (section 8.1), characteristic distances to natural faults are defined, over which stress perturbations are considered relevant for causing seismicity. These distances are based on expert judgement and refer to a typical geothermal facility. Characteristic distances should be used solely for the Quick-Scan. A more detailed analysis of the stress impact is required when planning a geothermal system in the tectonically active area in the Southeast of the Netherlands (Roer Valley rift system, e.g. Dost & Haak, 2007), where earthquakes with magnitudes M_L>5 have been registered (Figure 12).

Another important factor for assessing the seismic hazard associated with a geothermal facility is the occurrence of previously induced seismicity. Regions where induced seismicity has already occurred might still be in a near-critical stress state, where already minor stress perturbations may cause further seismicity.

In the Netherlands, induced seismicity is predominantly related to gas production, with most of the seismic activity being associated with the Groningen field (Figure 12).

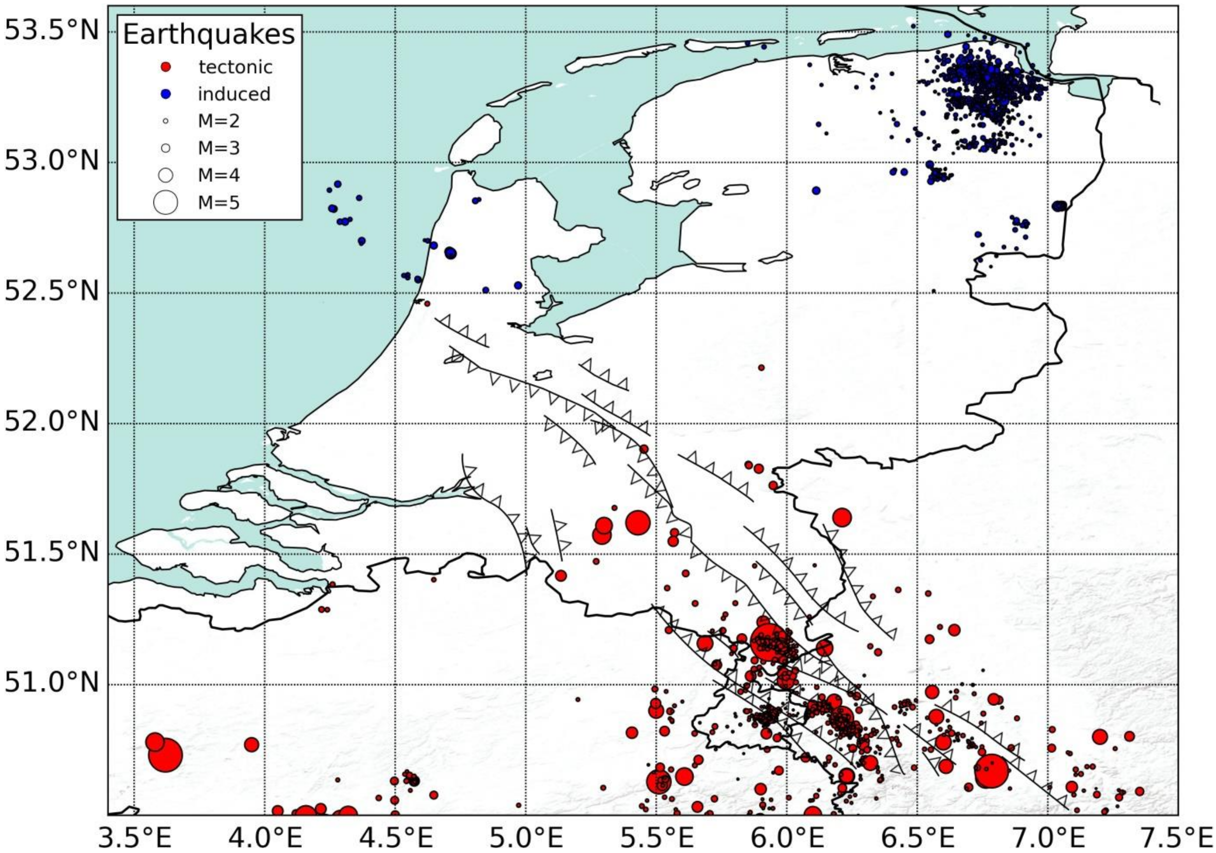

Figure 12: Natural (red) and induced (blue) seismicity in the Netherlands (KNMI catalogue as of March-2016, http://cdn.knmi.nl/knmi/map/page/seismologie). Symbol size is scaled to earthquake magnitude according to the legend. Fault trajectories of the Roer Valley rift system are indicated (data source: University of Utrecht, 2016).

6 EXISTING PRACTICE FOR HAZARD ASSESSMENT

The following sections briefly summarize how the induced seismicity hazard associated with geothermal facilities is addressed in selected countries. The focus of this overview is on requirements regarding a project specific seismic risk assessment and the operation of a traffic light system.

6.1 DOE Protocol

The Department of Energy (United States of America) released a protocol for addressing induced seismicity associated with Enhanced Geothermal Systems (Majer et al., 2012). Although designed for the US, the protocol has been referred to by other countries for outlining the general procedure.

The protocol suggests a seven step approach:

1. Performing a preliminary screening evaluation for the purpose of determining the overall feasibility of the project and identifying show-stoppers.
2. Implementing an outreach and communications program to engage the community in a positive and open manner before onsite activities begins.
3. Reviewing and selecting criteria for ground vibration and noise.
4. Establishing a local seismic monitoring system.
5. Quantifying the hazard from natural and induced seismic events.
6. Characterizing the risk of induced seismic events.
7. Developing a risk-based mitigation plan (traffic light system).

6.2 Germany

The legal framework for geothermal projects in Germany is given by the Federal Mining Act. Here, the exploitation of energy-supplying resources is assigned a privileged status. Minor damage due to seismicity related vibrations are to be accepted as long as structural damage can be ruled out.

The mining authorities of the different German provinces are responsible for approval procedures, which differ from state to state. For most facilities, a general environmental impact study is not required[3], but a quantitative assessment of the seismic hazard is frequently performed for the operational approval procedure. Several provinces require real-time seismic monitoring in combination with a traffic-light-system.

6.3 France

Geothermal projects in France require a general environmental impact study, but no separate seismic risk study is stipulated. Additionally, a special authorization by the French

[3] due to current changes in legislation an environmental impact study will be required in the future for certain types of geothermal systems/operations

authorities (*Prefecture*) is necessary. Operation of a traffic light system is generally not required.

6.4 Switzerland

Geothermal projects in Switzerland require a general environmental impact study, where induced seismicity risks are specifically addressed. Hydrothermal systems in Switzerland are operated without a traffic light system, whereas traffic light systems were operated during hydraulic operations in EGS projects.

7 RECOMMENDATION FOR HAZARD METRIC

Seismic hazard assessments are frequently based on peak ground vibrations (PGV) or on peak ground accelerations (PGA, or spectral acceleration, SA). For natural earthquakes, PGA is the most common metric. This is different for induced seismicity, where the focus is on higher frequency signals with short duration. For these, PGV is considered a better damage indicator than PGA (e.g. Bommer et al., 2006). Additionally, PGV can be directly compared to engineering standards, providing guidelines at what vibration level damage to buildings and other installations starts to occur. For example, damage to ordinary buildings is considered to be unlikely for PGV < 5 mm/s (SBR, 2010) and human perceptibility is expected to start at 0.3-0.5 mm/s.

Consistent with recommendations made in the DOE protocol (section 6.1), PGV is proposed as the most suitable metric for addressing seismic hazard associated with geothermal facilities in the Netherlands.

It is noted, however, that PGA might be a better metric for the Level 3 assessment (section 8.3), where the probabilistic framework requires the extrapolation of ground motion predictions towards larger magnitudes.

8 PROCEDURE RECOMMENDATION

In agreement with the draft guidelines for seismic hazard/risk assessment for natural gas fields (SodM, 2016), a three level approach is suggested. Level 1 (section 8.1) refers to a Quick-Scan for obtaining a rough estimate of the induced seismicity potential associated with geothermal operations. In case the Quick-Scan indicates medium or high potential for induced seismicity, a location-specific seismic hazard assessment (SHA) is required (section 8.2). Results of the SHA are incorporated into a qualitative risk matrix and it is decided whether or not a more detailed Level 3 seismic risk assessment (section 8.3) is required.

The following exceptions are defined, where at least a Level 2 assessment is required:

1. If the geothermal project is located close to a major fault zone (<100m) or if the exploration concept is based on circulating fluid through an existing fault, a Level 2 assessment is required independent of the results of the Quick-Scan.
2. If the geothermal project is located in the tectonically active area in the Southeast of the Netherlands (Roer Valley rift system).
3. If the geothermal project is located in the vicinity of the Groningen gas field, where subsurface stress conditions may be strongly altered by previous and ongoing gas production, a Level 2 assessment is required independent of the results of the Quick-Scan.

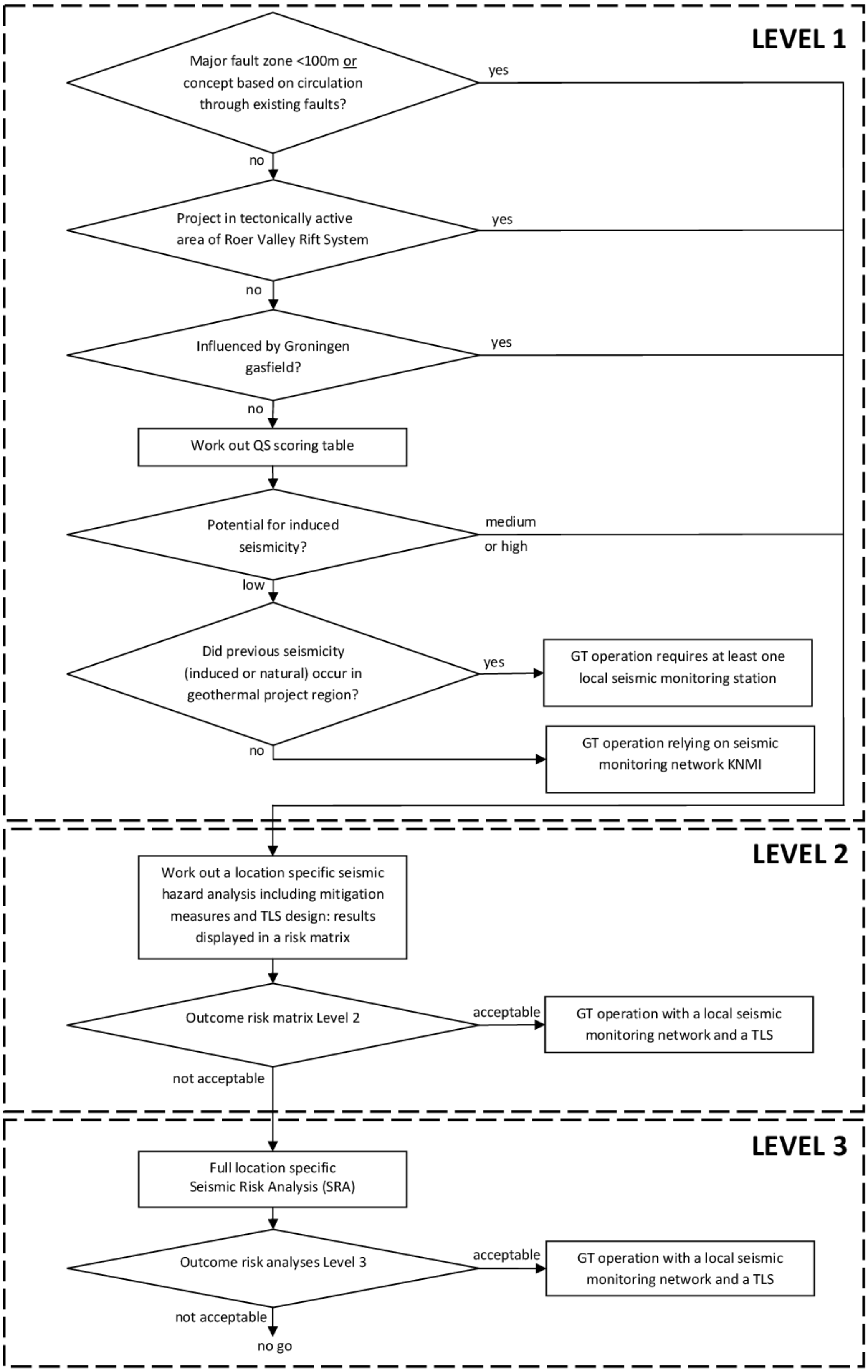

Figure 13: Decision tree for the three-level hazard and risk assessment procedure.

8.1 Level 1: Quick-Scan (QS)

The Quick-Scan screens the potential for inducing seismicity in a geothermal project. Based on the key parameters identified in chapter 5, a geothermal project is classified as having low, medium, or high potential for induced seismicity.

As noted previously, the occurrence of induced seismicity cannot be described by a single key parameter. It requires a combination of several necessary conditions and therefore the seismic hazard is controlled by parameter combinations rather than by a single parameter. Accordingly, the Quick-Scan is based on scores resulting from different parameters, with the three exceptions outlined in the previous section.

A scoring scheme as defined in Table 2 is proposed, where scores are assigned to certain key parameters. To apply the Quick-Scan to a geothermal project, scores from each key parameter are added and the total number is divided by the maximum possible number of scores (e.g. 90 if all parameters apply). This yields a normalized score in the range between 0 and 1. The induced seismicity potential is determined from the normalized score, where $S \geq 2/3$ indicates high, $1/3 < S < 2/3$ medium, and $S \leq 1/3$ low potential. Guidelines for assigning Quick-Scan scores are provided in Appendix A.

The Quick-Scan evaluates the overall project risk and does not distinguish between operations such as drilling, hydraulic stimulation, or circulation. Therefore, not all key parameters might be applicable in the planning phase of a geothermal project. Parameters which are not applicable are excluded from the Quick-Scan and the maximum possible number of scores is reduced accordingly. For example, if the Quick-Scan is applied to a geothermal exploration well, where no circulation operations are foreseen, then the parameters ‘circulation rate’ and ‘inter-well pressure communication’ need to be excluded and the maximum possible number of scores reduces to 70.

To evaluate the performance of the proposed scoring scheme, the Quick-Scan is applied to selected projects listed in section 4.2. The resulting potential for induced seismicity is compared to the maximum earthquake magnitude actually associated with the project (Figure 14). A good correlation between the Quick-Scan potential for induced seismicity and actual earthquake magnitude is obtained.

Two projects (Landau/Germany, Insheim/Germany) are assigned high seismicity potential, although these were only associated with moderate seismicity (Table 1). The high seismicity potential results from the design of these projects, which does not invoke a direct connection between injection and production wells. For the Landau system, the regulating authority placed a cap on production (and re-injection) rate after a felt earthquake has occurred.

score	basement connected	inter-well pressure communication	re-injection pressure [MPa]	circulation rate [m³/h]	epicentral distance to natural earth-quakes [km]	epicentral distance to induced seismicity [km]	distance to fault [km]	orientation of fault in current stress field	net injected volume [1000 m³]
10	yes	no	> 7	> 360	< 1	< 1	< 0.1	favorable	> 20
7	possible	unlikely	4 - 7	180-360	1 - 5	1 - 5	0.1 - 0.5	shearing possible	5 - 20
3	unlikely	likely	1 - 4	50-180	5 - 10	5 - 10	0.5 – 1.5	shearing unlikely	0.1 - 5
0	no	yes	< 1	< 50	> 10	> 10	> 1.5	locked	< 0.1

Table 2: Proposed scoring scheme for the Quick-Scan. 'Basement connected' refers to a hydraulic connection between injection well and the basement. 'Inter-well pressure communication' refers to the hydraulic connection between the injection and production wells. 'Distance to fault' refers to the distance between injection well and the nearest mapped fault. 'Orientation of fault in current stress field' refers to the orientation of the nearest mapped fault. 'Net injected volume' refers to the difference between injected and produced fluid volume. See Appendix A for further details.

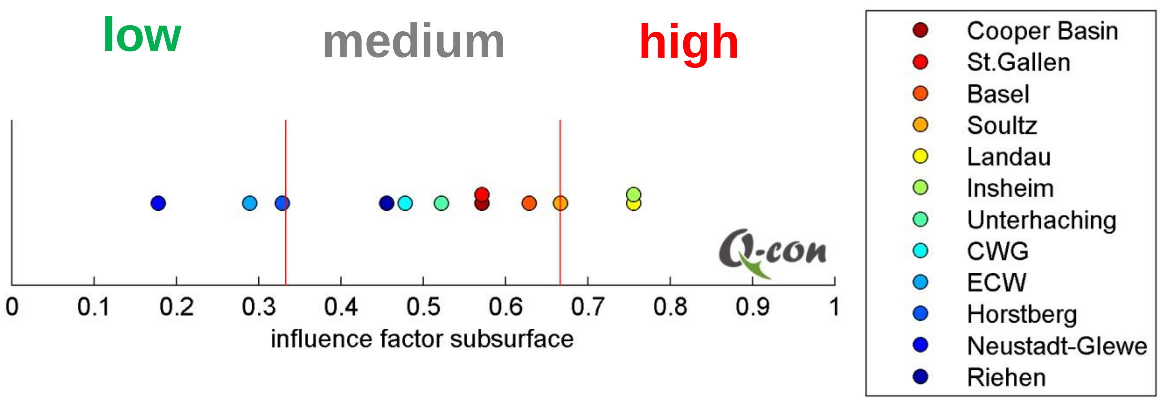

Figure 14: Quick-Scan applied to selected projects presented in section 4.2. Each colored dot represents the seismicity potential of a geothermal project as listed in the legend. Projects are sorted according to the maximum earthquake magnitude associated with the project, with the warm colors representing large magnitude, and cold colors representing no seismicity.

8.2 Level 2: Location-specific Seismic Hazard Assessment (SHA)

If the Quick-Scan (see previous section) yields a medium potential for induced seismicity, a location-specific seismic hazard assessment (SHA) is required.

The SHA should yield an estimate of the strength of induced seismicity associated with the planned geothermal operations in combination with an estimate of occurrence probabilities.

Classical seismic hazard assessments are typically based on the statistics of previous seismicity in a certain region (e.g. Cornell, 1968). This approach can usually not be applied in the planning phase for a geothermal system when no induced seismicity data is available. Alternative approaches are required, for which an example is presented in section 11.2.

The way a SHA is conducted may be very different. As a general guideline, any SHA should be conducted according to scientific standards. It should address the following key aspects (compare Barth et al., 2014):

- Description of the relevant physical processes that may cause seismicity in the project under consideration.
- Description of the geological and seismo-tectonic situation at the project location.
- Description of previous seismicity near the project location (natural, induced).
- Description of the planned subsurface operations.
- Justification of the methodology used for the hazard assessment.
- Seismic hazard assessment for the planned operations, e.g. drilling, hydraulic stimulation and fluid circulation.
- Identification of mitigation measures. These could include a cap on circulation rate, stopping, or even reversing an operation, e.g. producing from a previous injection well.
- Definition of a traffic light system (compare chapter 10) including the required response time for applying mitigation measures.

The results of the hazard assessment should be presented in a risk-matrix. For this, the number of buildings exposed to a certain vibration level needs to be estimated, which can be based on a ground motion prediction equation (GMPE). It is acknowledged that ground motion forecasts are subject to considerable uncertainty. In the context of the proposed Level 2 SHA, ground motion forecasts nevertheless provide a semi-quantitative measure for consequences.

Shake maps for earthquake scenarios can be compiled, e.g. using mean ground motion prediction models (e.g. Dost et al., 2004; Douglas et al., 2013), to identify buildings exposed to a certain vibration level. Subsequently, consequences are assigned according to the classification scheme presented in Table 3. Buildings with special character, either cultural or industrial, as well as dikes require an individual consideration if exposed to a vibration level ≥ 3 mm/s.

The proposed classification scheme (Table 3) is based on experience from a geothermal project underneath the city of Basel (Switzerland), where damage predictions were calibrated with observation data (Baisch et al., 2009). Using these calibrated functions it is estimated that

- minor consequences approximately correspond to a damage sum up to 10,000 Euros,
- moderate consequences approximately correspond to a damage sum up to 300,000 Euros,
- significant consequences approximately correspond to a damage sum up to several million to ten million Euros,
- and severe consequences imply a fatality risk.

It is acknowledged that these (mean) predictions are subject to large uncertainties and were derived for the specific settlement structure of Basel city. Clearly, settlement structures in the vicinity of a future geothermal project location in the Netherlands are likely to be different from those at Basel. However, the Basel observations represent a unique data set for a quantitative damage assessment in the geothermal industry. Therefore, it is used here for defining an initial classification scheme, which could be further refined if new observation data becomes available.

The risk matrix (Figure 15) shows consequences and their occurrence probability with color encoding denoting the acceptability of the seismic risk before and after mitigation. Green color indicates acceptable, red color unacceptable risks. Yellow color indicates that the risk is acceptable under certain conditions, i.e. the regulating authority decides if the risks appear acceptable in light of e.g. the project size, existing liability insurances and/or the financial body of the operator.

	Number of buildings exposed to PGV larger than			
consequence	3 mm/s	5 mm/s	20 mm/s	80 mm/s
negligible	0	0	0	0
minor	≤ 2,000	0	0	0
moderate		≤ 2,000	0	0
significant			≤ 500	0
severe				1

Table 3: Classification scheme for consequences. A consequence classification is assigned if all conditions in the associated line are fulfilled. If at least one condition is not fulfilled, the consequence category of the subsequent line applies. For example, if more than 2,000 buildings are exposed to PGV> 3mm/s, but none of the buildings is exposed to PGV > 5 mm/s, the consequences are classified as 'moderate'.

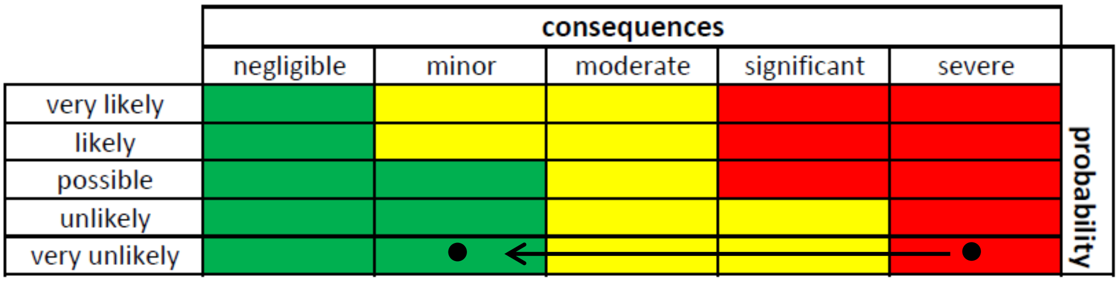

Figure 15: Risk matrix showing consequences and associated occurrence probabilities. Color encoding denotes risk acceptability with green=acceptable, yellow=acceptable under certain conditions, and red=unacceptable. The induced seismicity risk for a specific project is displayed by two points in the risk matrix indicating the total risk and the risk after mitigation.

8.3 Level 3: Location-specific Seismic Risk Assessment (SRA)

If the Quick-Scan (see section 8.1) yields a high potential for induced seismicity, a location-specific seismic risk assessment (SRA) is required. The SRA should quantitatively assess the economic and fatality risk associated with the planned geothermal project.

An SRA implies considerable more effort than the Level 2 SHA and it may not always be possible to quantify the risk within meaningful confidence limits because of parameter uncertainties. It is expected that projects classified as having a high potential for induced seismicity are usually not further pursued.

Even on a global scale, only few showcases exist where an SRA was performed for a geothermal project. Therefore, a detailed guideline for conducting an SRA cannot be given. In general, the same key aspects listed in the previous section need to be addressed by an SRA. However, a more thorough and detailed treatment of parameter estimates and their uncertainties is required, e.g. by conducting a probabilistic seismic risk analysis (PSRA).

Prior to project development, the lack of observation data is a complicating factor when conducting a PSRA. In particular, the forecast of the rate and strength of induced seismicity cannot be based on previous observations made at the geothermal site. Global data sets can be used to define the possible parameter range (e.g. Wong et al., 2010), but resulting hazard and risk are not strictly linked to the planned geothermal system (hazard estimates are independent of e.g. the circulation rate).

Examples of a PSRA conducted for geothermal operations are given by Baisch et al. (2009) and Mignan et al. (2014). Both studies are based on previously induced seismicity at the geothermal site.

9 RECOMMENDATIONS FOR SEISMIC MONITORING

Seismic monitoring of geothermal sites should provide robust measurements of the location and strength of local seismicity occurring near or inside a geothermal reservoir. These measurements form the basis for assigning seismicity to a certain reservoir (discrimination) and eventually for modifying or stopping geothermal activities (traffic light system).

9.1 Monitoring Network

The sensitivity and hypocenter location accuracy of a seismic monitoring network is basically determined by the number of monitoring stations and their spatial distribution as well as the type of instruments used.

For monitoring geothermal reservoirs, general recommendations are provided by Ritter et al. (2012):

1. A minimum number of 5 stations should be operated. An optimized station geometry depends on the number of stations included in the network and can be simulated as part of the network design. Nominal 2σ epicenter location errors should be at the level of +/- 500 m or less throughout the region of interest.
2. To facilitate the detection of secondary seismic waves, 3-component seismometers should be utilized.
3. The eigenfrequency of the seismometers should be ≤1 Hz.
4. The I95 noise level at the station locations should be ≤ 2,000 nm/s (vertical component) in the frequency range 5-40 Hz.
5. Seismometer recordings should be based upon an absolute time base (GPS synchronization).
6. The sampling frequency should be at least 100 Hz.
7. Data should be time continuously recorded and stored on a ≥24 bit acquisition system.
8. Real-time data access is required.

Additionally it is recommended to operate monitoring instruments at the Earth's surface to facilitate direct comparison of recordings to engineering standards.

To ensure compatibility with seismogram recordings from other operators (e.g. KNMI), it is recommended to use miniSEED as a common data format.

9.2 The KNMI Network

The Koninklijk Nederlands Meteorologisch Instituut (KNMI) operates a seismic station network for monitoring seismicity in the Netherlands. The station distribution is strongly heterogeneous with the highest station density in the Northeast and Southeast, respectively. Station configurations have changed repeatedly. As of 2010, the KNMI network exhibits a lower magnitude detection threshold of M_L=1.5 throughout most of the Netherlands except the Southwest (Figure 16). This implies that any earthquake with M_L > 1.5 occurring in the

Netherlands should generally be detected by the KNMI network. Similarly, earthquakes with M_L > 2.0 should generally be located by KNMI (Figure 17). Recent network extensions increased the station density significantly, in particular in the Groningen area (Figure 18).

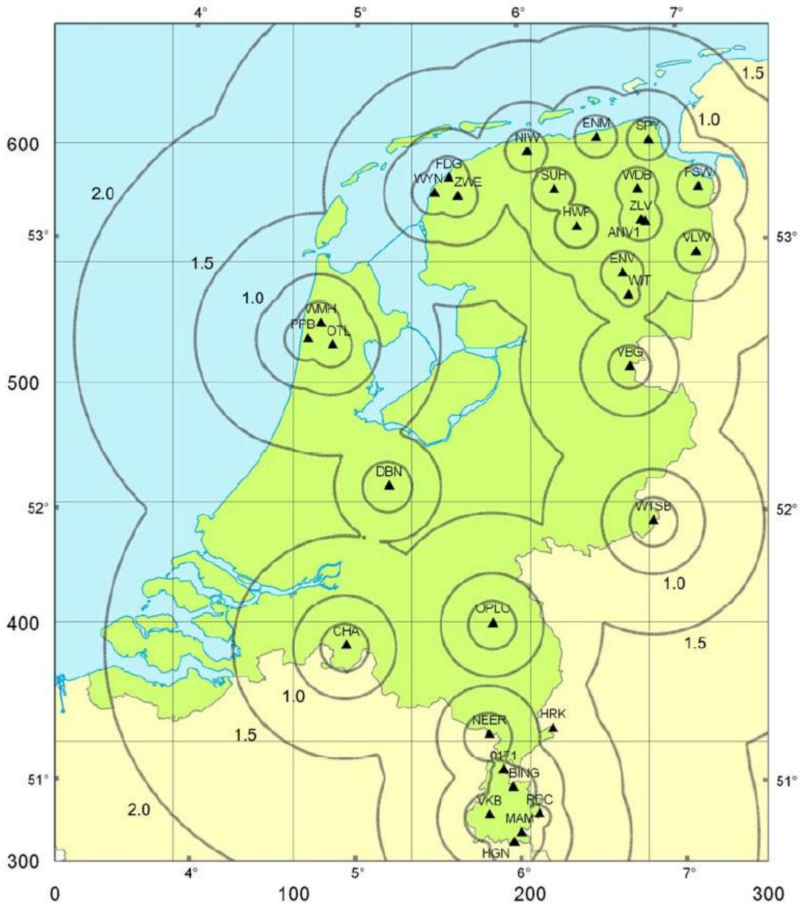

Figure 16: Lower magnitude detection threshold of the KNMI station network as of 2010. Figure taken from Dost et al. (2012). Contour lines indicate the minimum magnitude that can be detected with the KNMI station network.

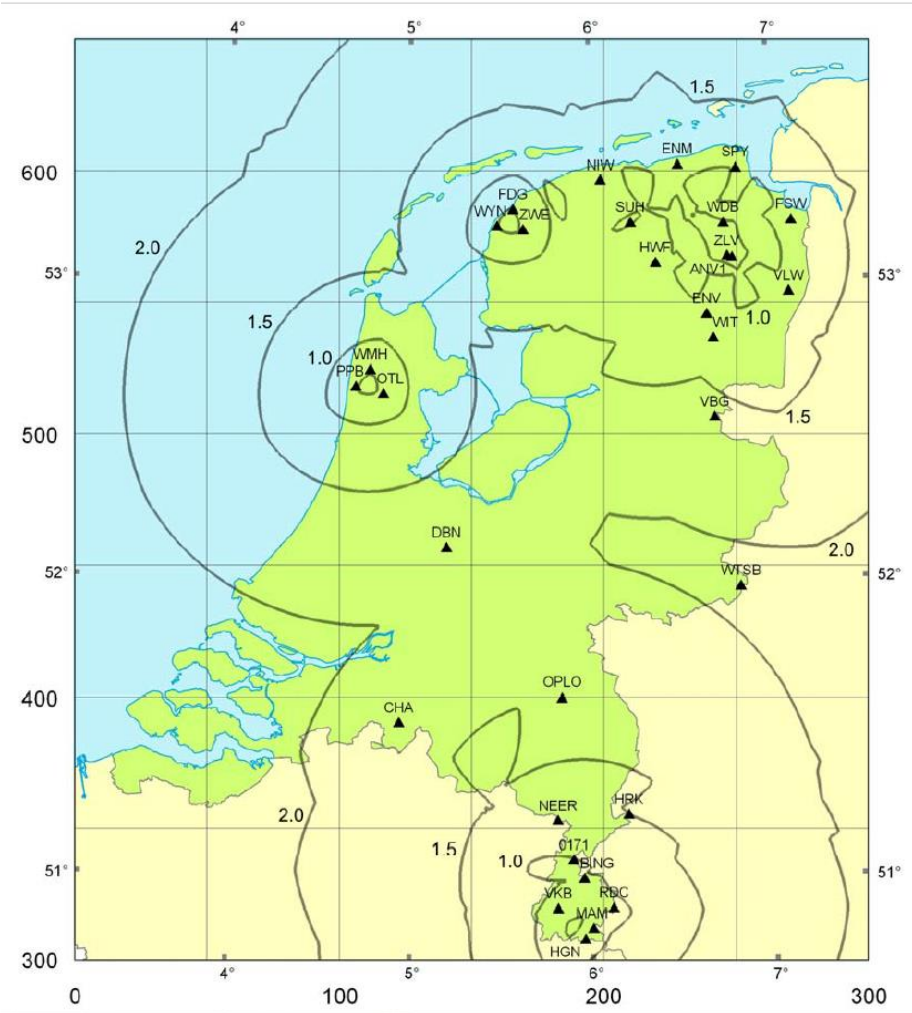

Figure 17: Lower location threshold of the KNMI station network as of 2010. Figure taken from Dost et al. (2012). Contour lines indicate the lowest magnitude of events for which hypocenters can be determined.

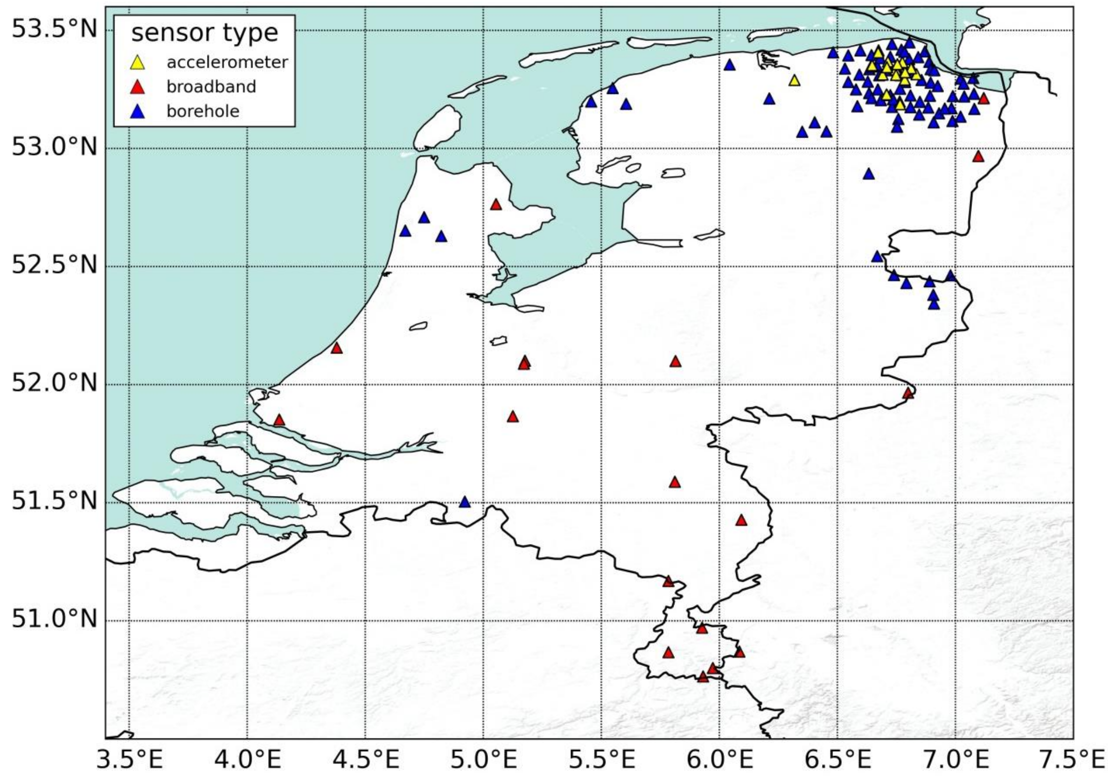

Figure 18: Location of recording stations operated by KNMI as of March 2016. Color encoding denotes different sensor types according to the legend. Data source: KNMI (http://www.knmi.nl/nederland-nu/seismologie/stations).

9.3 Requirements for Level 1 Scenario

The KNMI network and routine operations are considered sufficient for monitoring most geothermal systems classified as having low potential for inducing seismicity.

If previous seismicity has occurred in the geothermal project region or if the magnitude detection limit of the KNMI network is larger than M_w=1.5, an additional (single) local monitoring station close to a geothermal site might be required for discrimination purposes. The monitoring station needs to fulfill the technical requirements 2-8 of section 9.1.

9.4 Requirements for Level 2 and Level 3 Scenarios

In the medium and high hazard scenario, real-time monitoring plays an important role for risk mitigation. The KNMI network and routine operations usually cannot fulfill associated tasks and a dedicated local station network is required. The local station network should comply with the requirements 1-8 of section 9.1.

10 RECOMMENDATIONS FOR OPERATING A TRAFFIC LIGHT SYSTEM

The basis for operating a TLS as a risk mitigation measure (Bommer et al., 2006) is the characteristic increase of earthquake strength with duration of a geothermal operation (section 4.3).

As part of an SHA (section 8.2) or SRA (section 8.3), operational measures are defined which reduce the seismicity potential. Additionally, TLS threshold values are identified for applying mitigation measures.

A general challenge for the design of a TLS is a rapid magnitude increase as well as post-operational seismicity (section 4.4). These two effects need to be considered when defining TLS threshold values.

Following the recommendations made in chapter 7, TLS threshold values should be stated in terms of peak ground vibrations. Additional threshold values based on earthquake magnitude may be implemented, in which case the TLS status changes if either of the two threshold values (i.e. peak ground velocity threshold or magnitude threshold) is exceeded.

It is recommended that the TLS is operated solely by skilled and trained personal.

10.1 Level 1 Scenario

No TLS is operated in the low hazard scenario.

If an earthquake in the vicinity of a geothermal facility is detected by KNMI, the situation needs to be assessed by an expert group. It is proposed that the operator, KNMI and the regulating authority SODM are part of the expert group.

10.2 Level 2 Scenario

Depending on the outcome of the SHA, real-time monitoring in combination with a TLS may either be required for the entire lifetime of the geothermal system, or may be limited to certain project phases, e.g. when geomechanical subsurface conditions are highly non-stationary.

Less critical project phases do not necessarily require real-time monitoring. Depending on the previous seismicity response, the TLS may be operated with larger response times. The monitoring may even be handed over to KNMI if future seismicity appears unlikely in the geothermal reservoir.

It is proposed that an expert group is formed, including the operator, KNMI and the supervising authority SODM. Based on observation data, the expert group should propose to the supervising authority if less stringent requirements for TLS operation can be applied.

10.3 Level 3 Scenario

Real-time monitoring in combination with a TLS is required for the entire lifetime of the geothermal system.

Prior to geothermal operations, an expert group should be formed to address all issues associated with induced seismicity and to manage ‘unforeseeable’ events. It is proposed that the expert group includes the operator, KNMI, the regulating authority SODM, and one or more independent experts.

11 SHOWCASES

11.1 Middenmeer Geothermal Project

In the year 2013, ECW Geomanagement BV (ECW) started developing a geothermal system for heat production in Middenmeer (Figure 19). Reservoir target is the Slochteren formation and the geothermal system consists of two doublets, which are operated in a closed loop. Each doublet is designed for a circulation rate of approximately 80 l/s.

Table 4 shows the Quick-Scan applied to the ECW project. The normalized score indicates a low potential for induced seismicity, although near the transition to a medium potential. Following the recommendations in section 9.3, further (higher level) hazard assessment is not required and seismic monitoring by the KNMI station network would be sufficient. Due to the sparse KNMI station density in the project area, however, an additional (surface) seismometer station was deployed near the project location. This station was operated as a real-time detector during the initial 30 days of geothermal production until fluid overpressures in the subsurface were assumed to have reached quasi-stationary conditions. Thereafter, the station was integrated into the KNMI station network.

Seismic monitoring confirmed that geothermal operations at Middenmeer were not associated with induced seismicity even at a small magnitude level well below the human detection threshold.

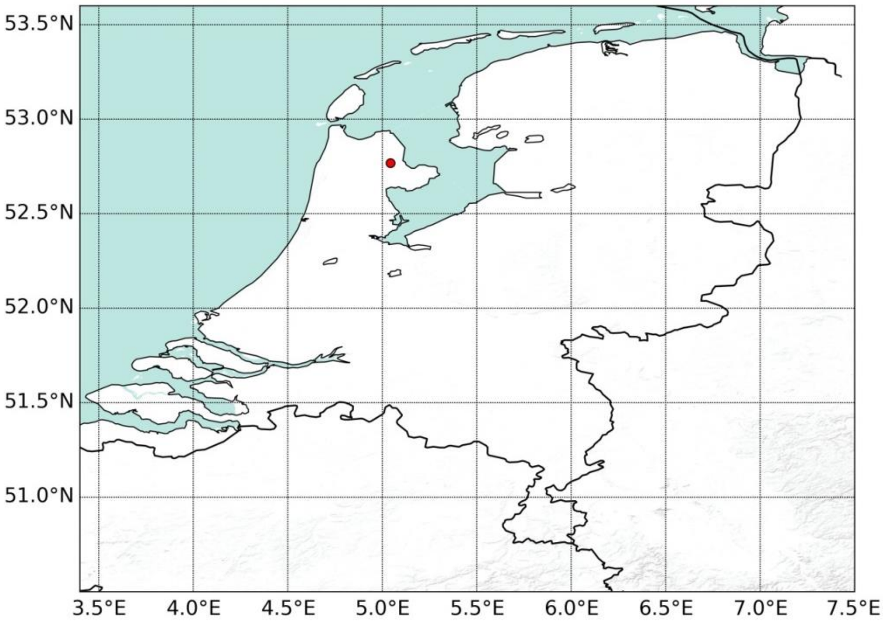

Figure 19: Location of the ECW geothermal project (red dot). For comparison, the detection threshold of the KNMI network at the project location is M_L=1.0 and the location threshold is M_L=1.5 (compare Figure 16 and Figure 17).

score	basement connected	inter-well pressure communication	re-injection pressure [MPa]	circulation rate [m³/h]	epicentral distance to natural earth-quakes [km]	epicentral distance to induced seismicity [km]	distance to fault [km]	orientation of fault in current stress field	net injected volume [1000 m³]
10	yes	no	> 7	> 360	< 1	< 1	< 0.1	favorable	> 20
7	possible	unlikely	4 - 7	180-360	1 - 5	1 - 5	0.1 - 0.5	shearing possible	5 - 20
3	unlikely	likely	1 - 4	50-180	5 - 10	5 - 10	0.5 - 1.5	shearing unlikely	0.1 - 5
0	no	yes	< 1	< 50	> 10	> 10	> 1.5	locked	< 0.1

Table 4: Level 1 Quick-Scan applied to the ECW project. The normalized Quick-Scan score is 0.29 indicating a low potential for induced seismicity.

11.2 Californie Geothermal Project

Californie Wijnen Geothermie (CWG) is operating a geothermal doublet near Venlo to supply greenhouses with heat. The reservoir formation is the Carboniferous Limestone Group and fluid is produced from the Tegelen fault zone that intersects the reservoir formation. The geothermal system has been operated since end 2013.

Table 5 shows the Quick-Scan applied to the CWG project. The normalized score indicates a medium potential for induced seismicity. Following the recommendations in section 9.3, a level 2 SHA is required.

Based on physical models, deterministic scenarios were numerically evaluated to assess the seismic hazard associated with the geothermal operations (Level 2 SHA). A slip-tendency analysis indicates that natural faults in the project area are potentially critically stressed. Based on operational parameters and geological conditions, numerical simulations of stress perturbations were conducted. These include stress changes associated with fluid overpressures, as well as changes induced by thermal cooling and the resulting contraction of reservoir rock. Simulation runs were performed for different scenarios including ‘extreme cases’. In all scenarios, Coulomb stress changes associated with hydraulic overpressures were found to be smaller than 0.1 MPa on mapped faults and were considered to be too small to induce noticeable seismicity.

Stress changes associated with thermal cooling were found to be < 0.1 MPa on all mapped faults except for the Tegelen fault. For the hypothetical case that the Tegelen fault responds seismically to these stress perturbations, it was demonstrated that seismicity strength slowly increases with time and escalation can be prevented by the traffic light system.

As a risk mitigation scheme, a seismic network for monitoring the geothermal system was installed and a traffic light system is operated with a stoplight in case reservoir seismicity causes ground vibrations in excess of 0.3 mm/s.

Figure 21 shows the risk matrix resulting from the Level 2 SHA before and after risk mitigation measures are applied.

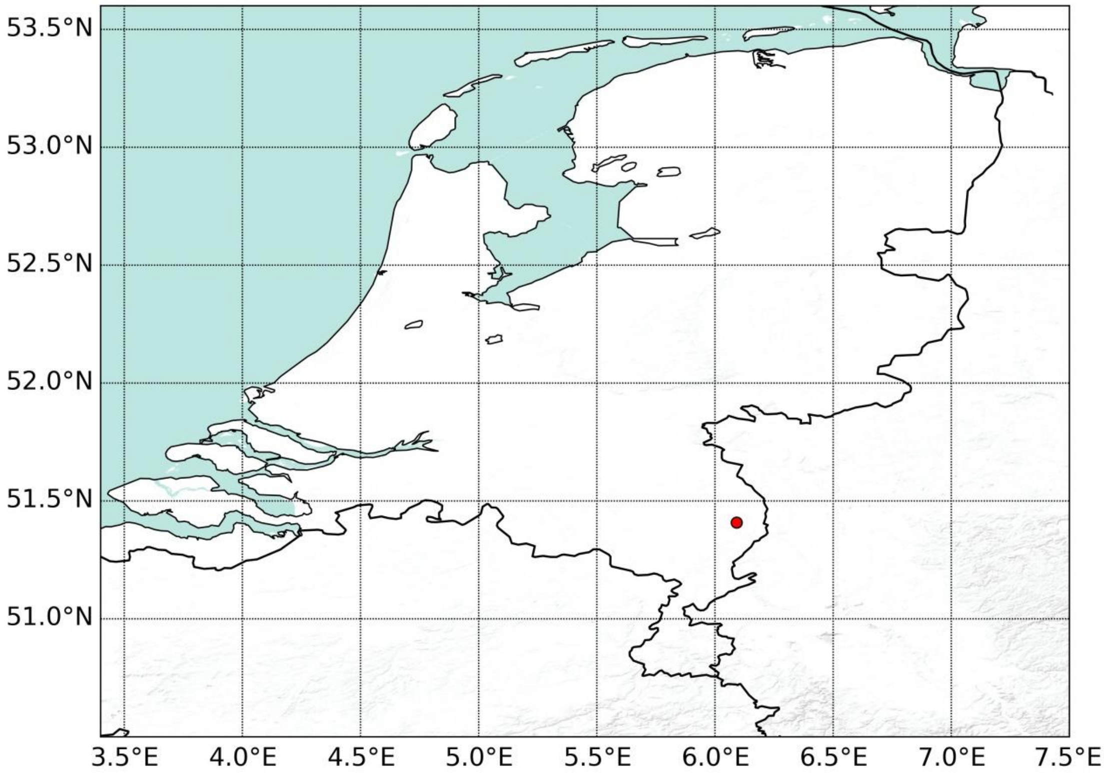

Figure 20: Location of the Californie geothermal project (red dot). For comparison, the detection threshold of the KNMI network at the project location is M_L=1.5 and the location threshold is M_L=2.0 (compare Figure 16 and Figure 17).

score	basement connected	inter-well pressure communication	re-injection pressure [MPa]	circulation rate [m³/h]	epicentral distance to natural earth-quakes [km]	epicentral distance to induced seismicity [km]	distance to fault [km]	orientation of fault in current stress field	net injected volume [1000 m³]
10	yes	no	> 7	> 360	< 1	< 1	< 0.1	favorable	> 20
7	possible	unlikely	4 - 7	180-360	1 - 5	1 - 5	0.1 - 0.5	shearing possible	5 - 20
3	unlikely	likely	1 - 4	50-180	5 - 10	5 - 10	0.5 – 1.5	shearing unlikely	0.1 - 5
0	no	yes	< 1	< 50	> 10	> 10	> 1.5	locked	< 0.1

Table 5: Level 1 Quick-Scan applied to the Californie project. The normalized Quick-Scan score is 0.48 indicating a medium potential for induced seismicity.

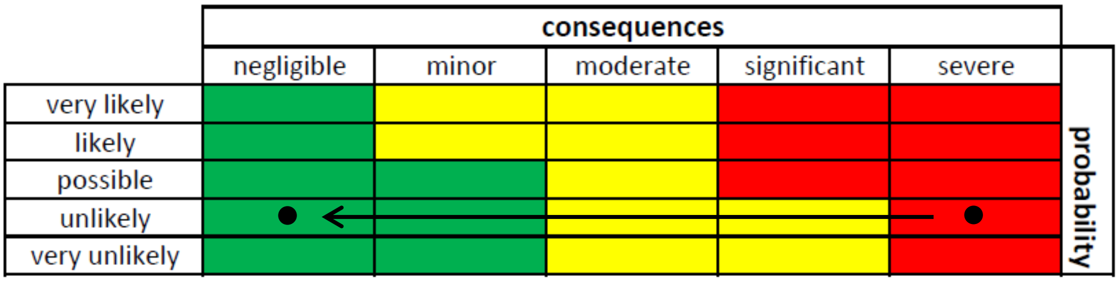

Figure 21: Risk matrix showing consequences and associated occurrence probabilities. Color encoding denotes risk acceptability with green=acceptable, yellow=acceptable under certain conditions, and red=unacceptable. The induced seismicity risk is characterized by the consequence-probability combinations (dots) of the overall seismic risk before and after applying mitigation measures.

REFERENCES

Abdullah, R. A., 2006. A study on stress-strain behaviour of granite and sandstone using closed-circuit servo-controlled testing machine. *Masters thesis*, Universiti Teknologi Malaysia.

Akkar, S., M.A. Sandıkkaya, and J.J. Bommer (2014). Empirical ground-motion models for point- and extended-source crustal earthquake scenarios in Europe and the Middle East. *Bulletin of Earthquake Engineering* **12**(1), 359-387.

Baisch, S., and H.-P.Harjes, 2003. A model for fluid injection induced seismicity at the KTB. *Geophys. Jour. Int.*, **152**, 160-170.

Baisch, S., Weidler, R., Vörös, R., Wyborn, D., and L. DeGraaf, 2006. Induced seismicity during the stimulation of a geothermal HFR reservoir in the Cooper Basin (Australia). *Bull. Seism. Soc. Amer.*, 96 (6), 2242-2256.

Baisch, S., Weidler, R., Vörös, R., and R. Jung, 2006b. A conceptual model for post-injection seismicity at Soultz-sous-Forêts. *Geothermal Resources Council*, Trans., Vol. 30, 601-606.

Baisch, S., Carbon, D., Dannwolf, U., Delacou, B., Devaux, M., Dunand, F., Jung, R., Koller, M., Martin, C., Sartori, M., Secanell, R., and R. Vörös, 2009. Deep Heat Mining Basel - Seismic Risk Analysis. *SERIANEX study prepared for the Departement für Wirtschaft, Soziales und Umwelt des Kantons Basel-Stadt, Amt für Umwelt und Energie*, 553 pages.

Baisch, S., Rothert, E., Stang, H., Vörös, R., Koch, C., and A. McMahon, 2015. Continued geothermal reservoir stimulation experiments in the Cooper Basin (Australia). *Bull. Seism. Soc. Amer.*, **105**, 198-209.

Baria, R., Michelet, S., Baumgärtner, J., Byer, B., Gerard, A., Nicholls, J., Hettkamp, T., Teza, D., Soma, N. Asanuma, H., Garnish, J., and T. Megel, 2004. Microseismic monitoring of the world's largest potential HDR reservoir. Proceedings, 29th Workshop on Geothermal Reservoir Enginerring, Stanford University, Stanford, California, January 26-28, 2004.

Barth, A., Schmidt, B., Joswig, M., Baisch, S., Fritschen, R., Gaucher, E., Kracht, M., Lehmann, K., Rüter, H., Schlittenhardt, J., and T. Spieß, 2014. Empfehlungen zur Erstellung von Stellungnahmen zur seismischen Gefährdung bei tiefengeothermischen Projekten - Positionspapier des FKPE, Oktober 2014. www.fkpe.org.

Boatwright, J., 1980. A spectral theory for circular seismic sources; simple estimates of source dimension, dynamic stress drop, and radiated energy. *Bull. Seism. Soc. Amer.*, **70**(1), 1-27.

Bommer, J. J., Oates, S., Cepeda, J. M., Lindholm, C., Bird, J., Torres, R., Marroquin, G., and J. Rivas, 2006. Control of hazard due to seismicity induced by a hot fractured rock geothermal project. Eng. Geol., 83, 287-306.

Bourne, S. J., and Oates, S., 2015. An activity rate model of seismicity induced by reservoir compaction and fault reactivation in the Groningen gas field. NAM report, 50 pages.

Brune, J., 1970. Tectonic stress and the spectra of seismic shear waves from earthquakes. *J., Geophys. Res.*, **75**, 4997-5009.

Cornell, C. A., 1968. Engineering Seismic Risk Analysis. *Bull. Seism. Soc. Amer.*, **58**, 1583 – 1606.

Costain, J. K. and Bollinger, G. A., 2010. Review: Research results in hydroseismicity from 1987 to 2009*. Bull. Seism. Soc. Amer.*, **100** (5), 1841-1858.

Deichmann, N., 2006. Local Magnitude, a Moment Revisited. *Bull. Seism. Soc. Amer.*, **96**, 1267 – 1277.

Deichmann, N., and D. Giardini, 2009. Earthquakes induced by the stimulation of an enhanced geothermal system below Basel (Switzerland). *Seis. Res. Let.*, 80, 784-798.

Dost, B., Van Eck, T., and H. Haak, 2004. Scaling of peak ground acceleration and peak ground velocity recorded in the Netherlands. *Bol. GeoF. Teo. Appl.*, **45**, 153-168.

Dost, B., and H. Haak , 2007. Natural and induced seismicity, in Geology of the Netherlands, ed. Wong, Batjes, de Jager, Royal Netherl. Acad. Arts & Sci., 223-239.

Dost, B., Goutbeck, F., van Eck, T.m, and D. Kraaijpoel, 2012. Monitoring induced seismicity in the North of the Netherlands, status report 2010. Internal document.

Douglas, J., Edwards, B., Cabrera, B. M., Convertito, V. Tramelli, A., Kraaijpoel, D., Maercklin, N., Sharma, N., and G. De Natale, 2013. Predicting Ground Motion from Induced Earthquakes in Geothermal Areas. Bull. Seism. Soc. Amer., doi:10.1785/0120120197.

Evans, K., Zappone, A., Kraft, T., Deichmann, N., and F. Moia, 2011. A survey of the induced seismic responses to fluid injection in geothermal and CO_2 reservoirs in Europe. *Geothermics*. doi:10.1016/j.geothermics.2011.08.002.

Geluk, M.C., Dusar, M., and W. de Vos, 2007. Pre-Silesian, in Geology of the Netherlands, ed. Wong, Batjes, de Jager, Royal Netherl. Acad. Arts & Sci., 27-42.

Ghassemi, A., Nygren, A. and Cheng, A. (2008). Effects of heat extraction on fracture aperture - A poro thermoelastic analysis. Geothermics vol. 37, pp. 525–539.

Hanks, T. C. and Kanamori, H., 1979. A moment magnitude scale. Jour. Geophys. Res., 84, 2348-2350.

Heidbach, O., Tingay, M., Barth, A., Reinecker, J., Kurfeß, D., Müller, B., 2009. The World Stress Map based on the database release 2008, equatorial scale 1:46,000,000. Commission for the Geological Map of the World, Paris, doi:10.1594/GFZ.WSM.Map2009.

de Jager, J., 2007. Geological development, in Geology of the Netherlands, ed. Wong, Batjes, de Jager, Royal Netherl. Acad. Arts & Sci., 5-26.

Majer, E., Nelson, J., Robertson-Tait, A., Savy, J., and I. Wong, 2012. Protocol for Addressing Induced Seismicity Associated with Enhanced Geothermal Systems. US Department of Energy, January 2012 | DOE/EE-0662, 52 pages.

McGarr, A., 1976. Seismic Moment and Volume Change. Jour. Geophys. Res., **81**, 1487-1494.

McGarr, A., 2014. Maximum magnitude earthquakes induced by fluid injection. J. Geophys. Res. Solid Earth, **119**, doi:10.1002/2013JB010597.

Mignan, A., Landtwing D., Kästli P., Mena B., and S. Wiemer, 2014. Induced seismicity risk analysis of the 2006 Basel, Switzerland Enhanced Geothermal System project: Influence of uncertainties on risk mitigation. *Geothermics*, **53**, 133-146.

Mulders, F.M.M. (2003). Modelling of Stress Development and Fault Slip in and Around a Producing Gas Reservoir. Doctoral thesis, Technical University of Delft, Delft.

National Research Council, 2012. Induced Seismicity Potential in Energy Technologies. National Academies Press, Washington, D.C, ISBN 978-0-309-25367-3, 226 pages.

Parotidis, M., Shapiro, S. A., and E. Rothert, 2004. Back front of seismicity induced after termination of borehole fluid injection. Geophys. Res. Let., 31, L02612, doi:10.1029/2003GL018987.

Ritter, J., Baisch, S., Fritschen, R., Groos, J., Kraft, T., Plenefisch, T., Plenkers, K., Wassermann, J., 2012. Empfehlungen zur Überwachung induzierter Seismizität - Positionspapier des FKPE. Mitteilungen der Deutschen Geophysikalischen Gesellschaft e.V., Nr. 3/2012, ISSN 0934-6554, pages 17-31.

SBR, 2010. Schade aan Gebouwen, Deel A uit de Meet– en beoordelingsrichtijn: Trillingen.

Scholz, C. H., 2002. The Mechanics of Earthquakes and Faulting. Cambridge University Press, 2nd Edition.

Segall, P. and Fitzgerald, S.D. (1998). A note on induced stress changes in hydrocarbon and geothermal reservoirs. *Tectonophysics*, **289**, pp. 117-128.

Shapiro, S., Huenges, E., and G. Borm, 1997. Estimating the crust permeability from fluid-injection-induced seismic emission at the KTB site. *Geophys. J. Int.*, **131**, F15-F18.

SodM, 2016, Methodiek voor risicoanalyse omtrent geïnduceerde bevingen voor gaswining - Tijdelijke leidraad voor adressering MBB. 224.1.P, versie 1.2.

Townend, J., and Zoback, M., 2000. How faulting keeps the crust strong. *Geology*, **28 (5)**, 399-402.

University of Utrecht, 2016. „Thickness of the Quarternary (m) in the Netherlands“, *http://www.geo.uu.nl/fg/palaeogeography/pictures/delta_history/04-Thickness-Quaternary.png,* downloaded 11.05.2016.

Van Eijs, R.M.H.E., Mulders, F. M. M., Nepveu, M., Kenter, C. J., and B.C. Scheffers, 2006. Correlation between hydrocarbon reservoir properties and induced seismicity in the Netherlands. Engineering *Geology,* **84**, 99-111.

van Thienen-Visser, K., Nepveu, M. and Hettelaat, J. (2012). Deterministische hazard analyse voor geïnduceerde seismiciteit in Nederland. TNO-report 2012 R10198.

van Wees, J.D., Buijze L., van Thienen-Visser, K., Nepveu, M., Wassing, B., Orlic, B. and Fokker, P.A. (2014). Geomechanics response and induced seismicity during gas field depletion in the Netherlands. *Geothermics*, **52**, pp. 206-219.

White, J.A., and Foxall, W. (2014). A phased approach to induced seismicity risk management. Energy Procedia 63 (2014) 4841 – 4849.

Wong, I., Pezzopane, S., Dober, M., and F. Terra, 2010. Evaluations of induced seismicity / Seismic Hazards and Risk for the Newberry Volcano EGS Demonstration Plant. URS report prepared for AltaRock Energy Inc., 106 pages.

Zoback, M. D., 2007. Reservoir Geomechanics. Cambridge University Press, Cambridge, New York, ISBN-978-0-521-77069-9.

APPENDIX A : ASSIGNING QUICK-SCAN SCORES

The Level 1 Quick-Scan is applied in the planning phase of a geothermal project. At this stage, the knowledge of subsurface conditions is inherently incomplete. Therefore, the Quick-Scan is based on the best available information.

If multiple answers can be given to a certain parameter (-combination), then the parameter (-combination) with the largest score applies. For example, consider two natural faults near the project location. The trajectory of fault A runs at a distance < 0.1 km to the injection well (10 scores), but is oriented such that it is likely to be locked in the current stress field (0 scores). The closest part of Fault B is at a distance of 700 m (3 scores) and is oriented favorable for shearing in the current stress field (10 scores). In this case, Fault B needs to be considered in the Quick-Scan because of the larger scoring associated with it.

Guidelines for assigning scores to all key parameters defined in chapter 5 are provided in the subsequent sections.

A.1. Hydraulic connection to crystalline basement

- Score = 10 when the geothermal system targets the crystalline basement.
- Score = 7 when it is possible that the vertical separation between the geothermal reservoir and the crystalline basement is ≤1.5 km.
- Score = 3 when it is possible that the vertical separation between the geothermal reservoir and the crystalline basement is ≤3.0 km.
- Score = 0 when the vertical separation between the geothermal reservoir and the crystalline basement is > 3.0 km.

A.2. Distance to natural faults

The distance to natural faults refers to the minimum distance of the (open hole section of the) injection well to a mapped fault trace. Fault traces can be derived from seismic data interpretation or from regional tectonic maps. The fault thickness needs to be accounted for when estimating distances. For faults exhibiting a significant thickness (process or fault zone), distance estimates need to be reduced accordingly.

- Score = 10 when distance to faults < 0.1 km or when seismic data is poor (wells intersecting a significant fault cannot be excluded).
- Score = 7 when distance to faults is 0.1-0.5 km or when the accuracy of the interpreted seismic data is limited (undetected significant faults may be possible).
- Score = 3 when distance to faults is 0.5-1.5 km and when the accuracy of the interpreted seismic data is reasonable.
- Score = 0 when distance to faults > 1.5 km according to high quality 3D seismic data.

A.3. Fault orientation in stress field

The orientation of the stress field can be derived from break-out analyses and/or the world stress map (Heidbach et al., 2009). The orientation of faults is based on seismic data interpretation or regional maps. The orientation of the local stress field as well as the fault orientation is subject to uncertainty. Therefore, a qualitative scoring scheme is proposed:

- Score = 10 when the fault is oriented favourable for shear in the regional stress field.
- Score = 7 when shearing on the fault appears possible in the regional stress field.
- Score = 3 when shearing on the fault appears unlikely in the regional stress field.
- Score = 0 when the fault trajectory is orthogonal to the maximum stress direction of the regional stress field.

A.4. Distance to natural earthquakes

The basis for determining distances to natural earthquakes is the most recent earthquake catalogue published by KNMI (*www.knmi.nl*). It is acknowledged that the hypocentral depth of earthquakes in the KNMI catalogue is generally less well constrained than the epicentral coordinates. Therefore, earthquake depth is not considered and the scoring scheme is based on epicentral distance. The uncertainty of the epicentral coordinates in the KNMI catalogue is depending on data quality and on the location, where in the Netherlands the earthquake occurred. Typical epicentral location errors are between 1 km and 5 km. These uncertainties are accounted for in the scoring scheme.

The epicentral distance is determined as the lateral distance between the injection well (center of the open hole section) and the catalogued epicenter of an earthquake. For the Quick-Scan, the epicentral distance of the closest earthquake is considered.

- Score = 10 when the epicentral distance to a natural earthquake < 1 km.
- Score = 7 when the epicentral distance to a natural earthquake is between 1 km and 5 km.
- Score = 3 when the epicentral distance to a natural earthquake is between 5 km and 10 km.
- Score = 0 when distance to the closest natural earthquake is > 10 km.

A.5. Distance to induced seismicity

The basis for determining distances to induced earthquakes is the most recent earthquake catalogue published by KNMI (*www.knmi.nl*). It is acknowledged that the hypocentral depth of earthquakes in the KNMI catalogue is generally less well constrained than the epicentral coordinates. Therefore, earthquake depth is not considered and the scoring scheme is based on epicentral distance. The uncertainty of the epicentral coordinates in the KNMI catalogue is depending on data quality and on the location, where in the Netherland the earthquake occurred. Typical epicentral location errors are between 1 km and 5 km. These uncertainties are accounted for in the scoring scheme.

The epicentral distance is determined as the lateral distance between the injection well (center of the open hole section) and the catalogued epicenter of an earthquake. For the Quick-Scan, the epicentral distance of the closest induced earthquake is considered.

- Score = 10 when the epicentral distance to an induced earthquake < 1 km.
- Score = 7 when the epicentral distance to an induced earthquake is between 1 km and 5 km.
- Score = 3 when the epicentral distance to an induced earthquake is between 5 km and 10 km.
- Score = 0 when distance to the closest induced earthquake is > 10 km.

A.6. Net injected volume

Fluid injection is relevant during different phases of developing and operating a geothermal system.

i. Smaller amounts of fluid are injected during acidizing and reservoir testing, in which case the net injected volume equals the injected volume.
ii. Larger amounts of fluid are injected for hydraulically stimulating reservoirs, in which case the net injected volume equals the injected volume.
iii. During mass-balanced fluid circulation (i.e. produced volume equals re-injected volume) the net injected volume is zero (compare the definition in section 5.2.1).

The Quick-Scan scores refer to the operation that invokes the largest fluid volume. Operations may last over a longer period of time and it may be difficult to determine the point in time when a certain operation is completed and when the subsequent operation begins. As a guideline, an operation is considered complete when fluid injection is interrupted long enough for the reservoir pressure to return to equilibrium.

- Score = 10 when the net injected volume is > 20,000 m^3.
- Score = 7 when the net injected volume is 5,000 – 20,000 m^3.
- Score = 3 when the net injected volume is 100 – 5,000 m^3.
- Score = 0 when the net injected volume is < 100 m^3.

A.7. Inter-well pressure communication

Inter-well pressure communication can be blocked or hindered, when the injection and production wells are separated by a hydraulic barrier. This barrier can be a layer with a low permeability in the reservoir itself (when production and injection takes place above and below that layer), a confining layer (when the wells are intentionally placed in different reservoirs) or a fully or partially sealing fault (when the wells use different reservoir blocks/compartments).

Most geothermal systems are designed to have a reasonable hydraulic connection between injection and production wells. The likelihood that hydro-geological barriers or hydraulic friction unintentionally reduce pressure communication scales with the inter-well separation. This is reflected in the scoring scheme.

- Score = 10 when the injection and production wells are designed to have no pressure communication.
- Score = 7 when the (open hole sections of the) injection and production wells
  - are targeting different geological formations,
  - or are laterally separated by > 2,000 m,
  - or are vertically separated by > 500 m.
- Score = 3 when the (open hole sections of the) injection and production wells
  - are targeting the same formation,
  - and are laterally separated by 1,000 - 2,000 m,
  - and are vertically separated by 100 m - 500 m.
- Score = 0 when the (open hole sections of the) injection and production wells
  - are targeting the same formation,
  - and are laterally separated by < 1,000 m,
  - and are vertically separated by < 100 m.

A.8. Re-injection pressure

The re-injection pressure refers to the expected overpressure applied at reservoir level when the geothermal system is operated at its full capacity. Usually, the re-injection pressure is estimated as part of the business plan.

It is assumed that the re-injection pressure will always remain below the fracture propagation pressure due to requirements of the supervising authority.

- Score = 10 when expected re-injection pressure > 7 MPa.
- Score = 7 when expected re-injection pressure is 4-7 MPa.
- Score = 3 when expected re-injection pressure is 1-4 MPa.
- Score = 0 when expected re-injection pressure is <1 MPa.

A.9. Circulation rate

This parameter refers to the circulation rate when the geothermal system is operated at its full capacity. Usually, maximum circulation rate is a design parameter of the geothermal system.

- Score = 10 when circulation rate > 360 m^3/h.
- Score = 7 when circulation rate is 180-360 m^3/h.
- Score = 3 when circulation rate is 50-180 m^3/h.
- Score = 0 when circulation rate < 50 m^3/h.